united nations
educational, scientific
and cultural
organization

international atomic
energy agency

the
abdus salam
international centre for theoretical physics

SMR.1313 - 9

Summer Colloquium on the Physics of Weather and Climate

Workshop on
Land-Atmosphere Interactions in Climate Models
(28 May - 8 June 2001)

Atmospheric Impacts of Surface Variability

Christopher M. Taylor
Centre for Ecology and Hydrology Wallingford
Crowmarsh Gifford, Oxfordshire
OX10 8BB Wallingford
U.K.

These are preliminary lecture notes, intended only for distribution to participants

Atmospheric Impacts of Surface Variability

(i) Diurnal timescale and 1D Feedbacks

(ii) Rainfall Persistence during HAPEX-Sahel

(iii) Synoptic Variability – African Easterly Waves

Reference List

1. Albignat JP, Reed RJ: The origin of African wave disturbances during phase III of GATE. Mon.Weath.Rev. 1980;108:1827-1839.

2. Betts AK, Ball JH: FIFE surface climate and site-average dataset 1987-89. J.Atmos.Sci. 1998;55:1091-1108.

3. De Ridder K: Land surface processes and the potential for convective precipitation. J.Geophys.Res.Atmos. 1997;102:30085-30090.

4. Ek M, Mahrt L: Daytime evolution of relative humidity at the boundary layer top. Mon.Weath.Rev. 1994;122:2709-2721.

5. Eltahir EAB: A soil moisture-rainfall feedback mechanism 1. Theory and observations. Wat.Resour.Res. 1998;34:765-776.

6. Findell KL, Eltahir EAB: An analysis of the soil moisture-rainfall feedback, based on direct observations from Illinois. Wat.Resour.Res. 1997;33:725-735.

7. Reed, R. J., Norquist, D. C., and Recker, E. E. The structure and properties of African wave disturbances as observed during phase III of GATE. Monthly Weather Review 105, 317-333. 1977.

8. Taylor CM, Saïd F, Lebel T: Interactions between the land surface and mesoscale rainfall variability during HAPEX-Sahel. Mon.Weath.Rev. 1997;125:2211-2227.

9. Taylor CM, Lebel T: Observational evidence of persistent convective-scale rainfall patterns. Mon.Weath.Rev. 1998;126:1597-1607.

10. Taylor CM: The influence of antecedent rainfall on Sahelian surface evaporation. Hydrol.Processes 2000;14:1245-1259.

11. Taylor CM, Clark DB: The diurnal cycle and African easterly waves: a land surface perspective. Quart.J.Roy.Meteorol.Soc. 2000;127:845-868.

12. Thorncroft CD, Rowell DP: Interannual variability of African wave activity in a general circulation model. Int.J.Climatol. 1998;18:1305-1323.

I Diurnal Timescale

radiosounding observations from HAPEX-Sahel

an example of a well-mixed convective boundary layer

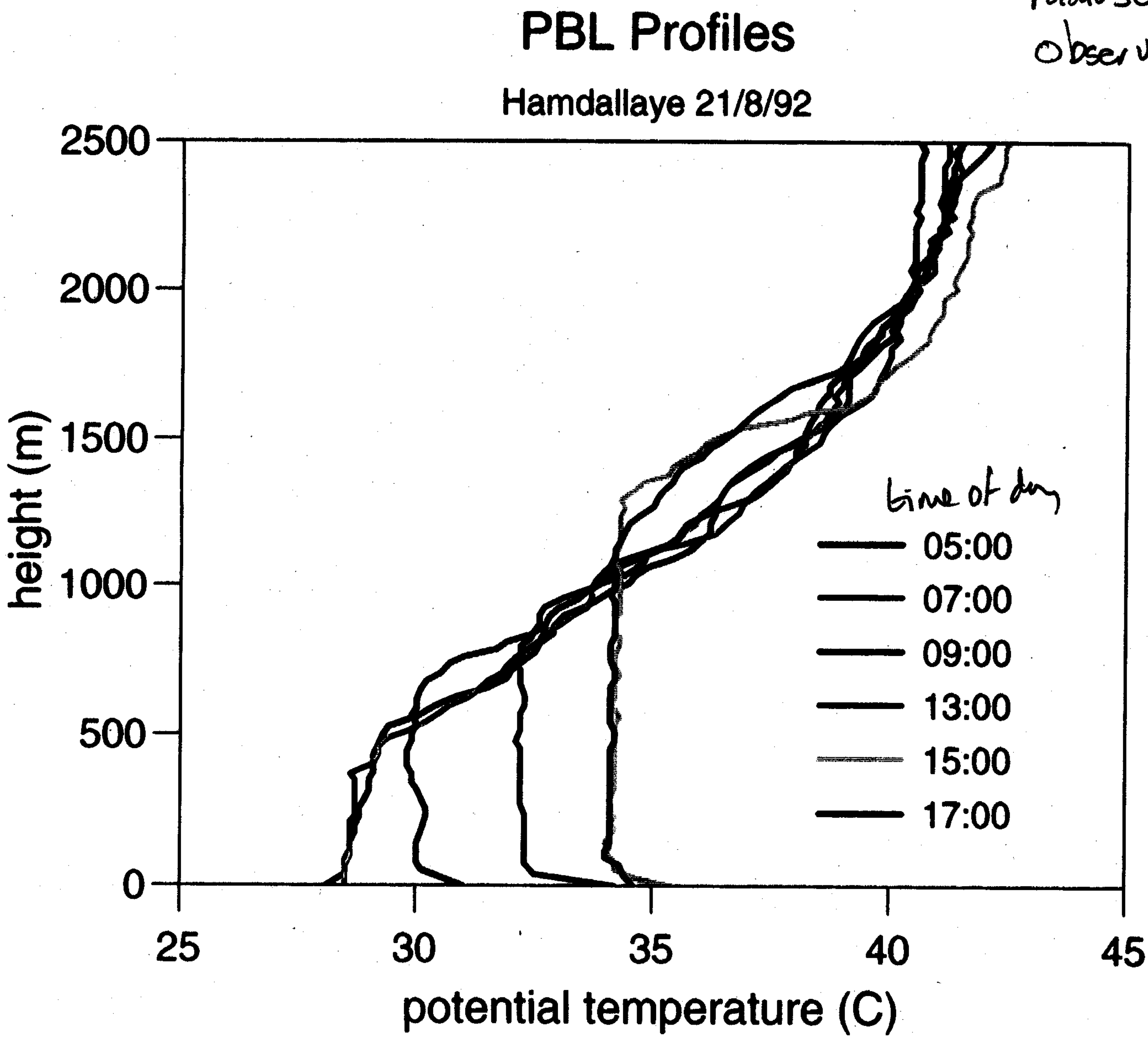

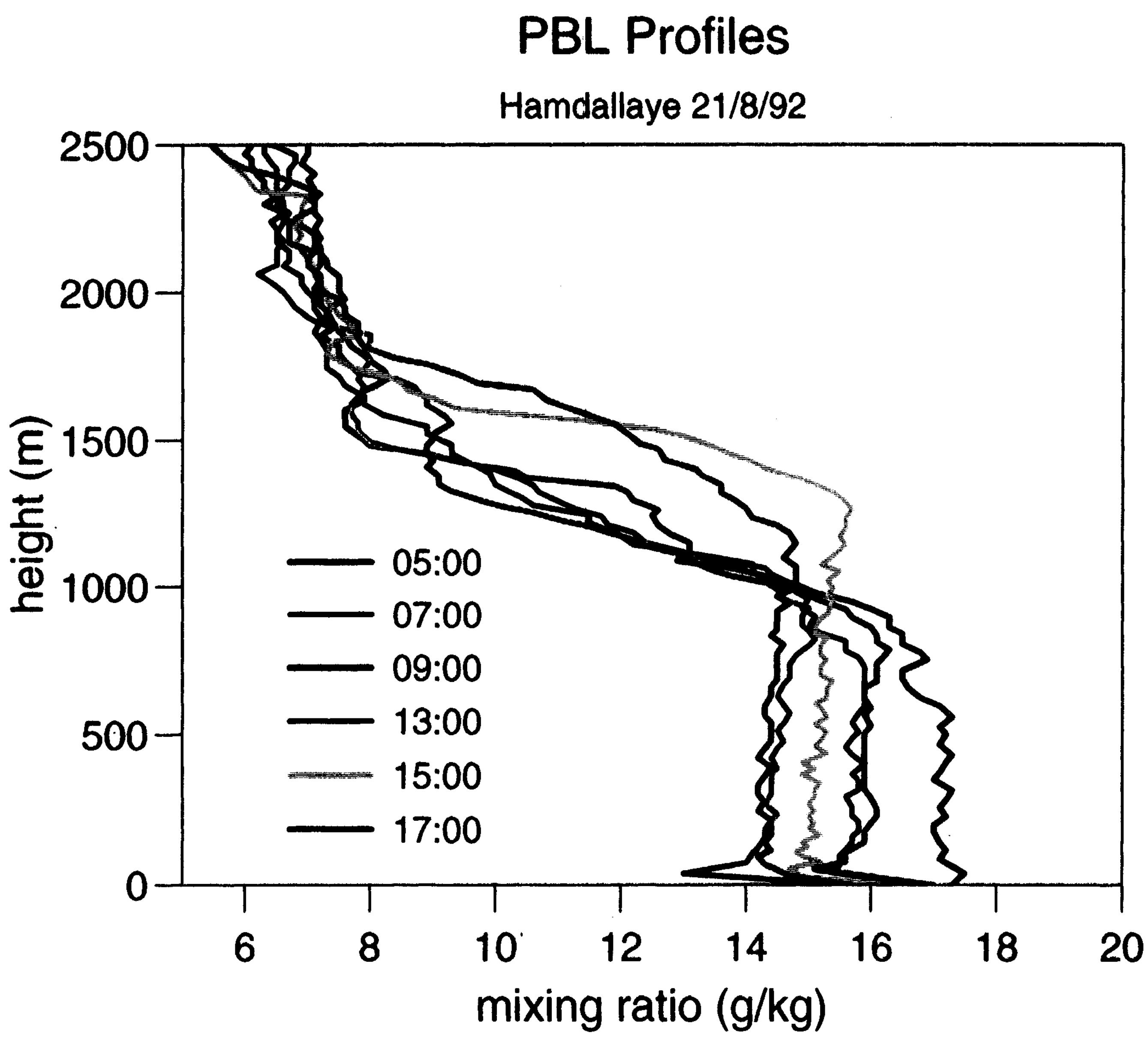

PBL Profiles
Hamdallaye 21/8/92
2500
2000
1500
1000
500
0
height (m)
05:00
07:00
09:00
13:00
15:00
17:00
6
8
10
12
14
16
18
20
mixing ratio (g/kg)

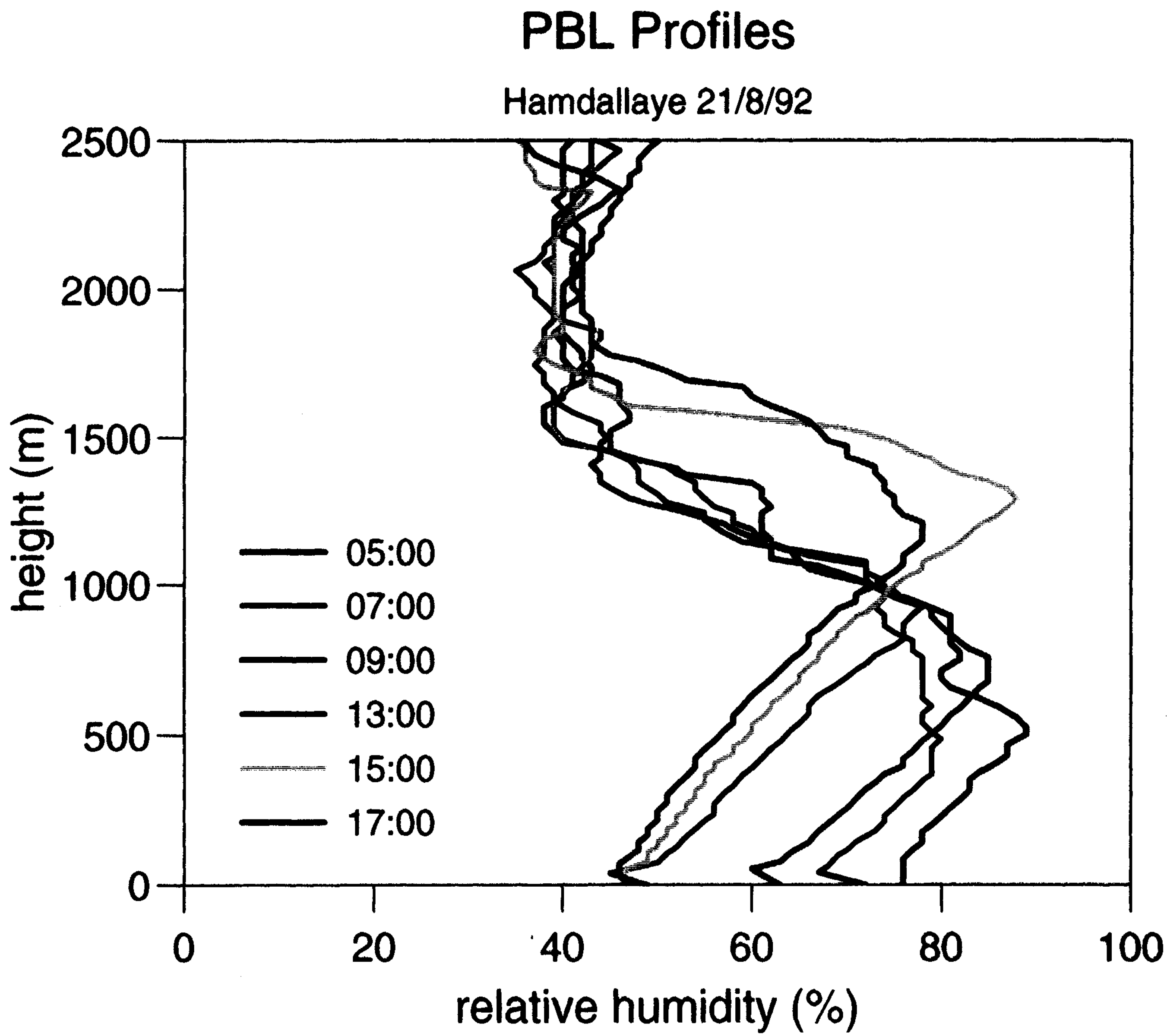
PBL Profiles
Hamdallaye 21/8/92
2500
2000
1500
1000
500
0
height (m)
05:00
07:00
09:00
13:00
15:00
17:00
0
20
40
60
80
100
relative humidity (%)

clearly, surface fluxes drive diurnal cycle of PBL

question:
how does a change in fluxes affect stability of profile to moist convection

various studies eg Ek + Mahrt, Betts + Ball, de Ridder

show that higher evaporative fraction should usually → more frequent + more intense convection

when considering no feedbacks, dynamics etc

GCM experiment to illustrate processes on diurnal timescale

Unified Model HadAM3 version

surface parameters in Sahel are unrealistic

- high LAI, low albedo, low soil fraction, poor drainage...
- derived from Wilson + Henderson-Sellers
- acts like densely vegetated, well-watered surface

what happens on diurnal scale in GCM if ~~more~~ realistic parameters introduced over Sahel?

(this experiment is described in Taylor + Clark 2001) standard parameters

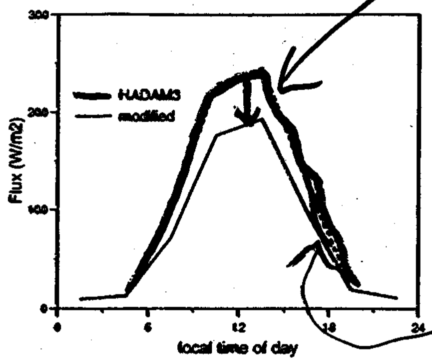

evaporation
decrease ~50 Wm^{-2}

improved parameters

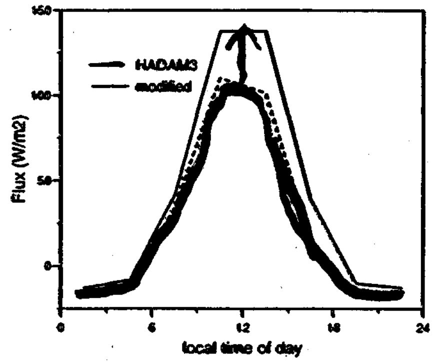

sensible heat
increase ~ 30 Wm^{-2}

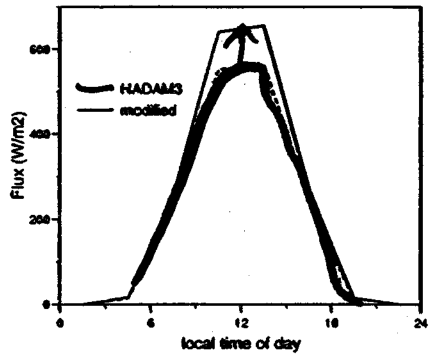

incoming s.w.
increase ~ 100 Wm^{-2}

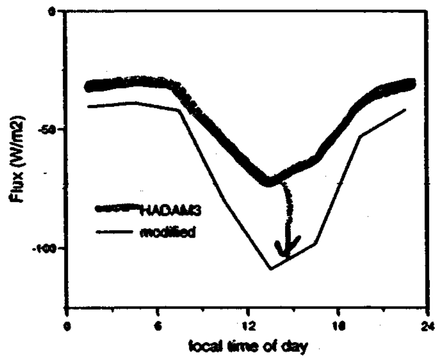

outgoing l.w.
increase ~30 Wm^{-2}

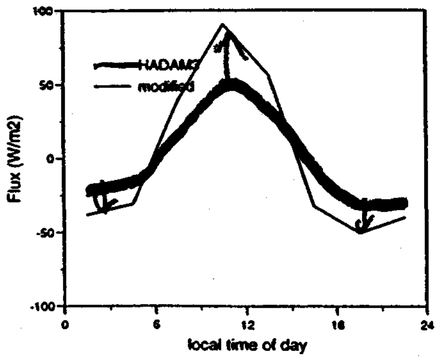

soil heat flux
amplitude increased ~ 75 [illegible]

JAS mean

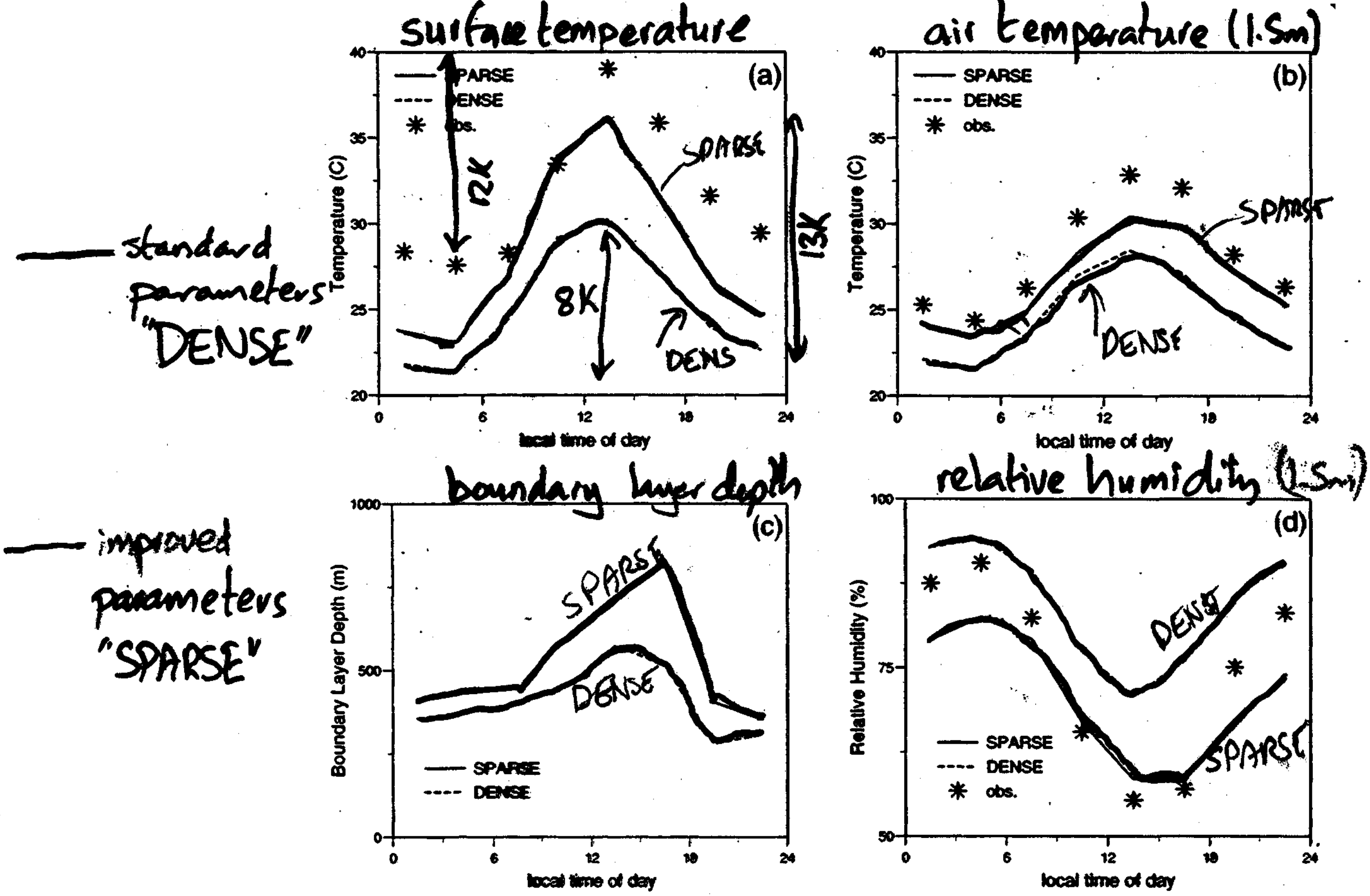

Figure 7. As Fig. 5 but for: (a) surface temperature (°C), (b) temperature at 1.5 m (°C), (c) boundary-layer depth (m), and (d) relative humidity at 1.5 m (%). Also shown for comparison are July to September mean observations over two years from a savanna field site (13.5°N, 2.7°E) of soil temperature at 2 cm depth in (a), of 2 m air temperature in (b), and of 2 m relative humidity in (d).

likelihood of PBL driven convection in model?

SPARSE has lower RH at surface → less convection

BUT

PBL is deeper ∴ top of mixed layer is cooler, + q_{sat} is lower → more convection

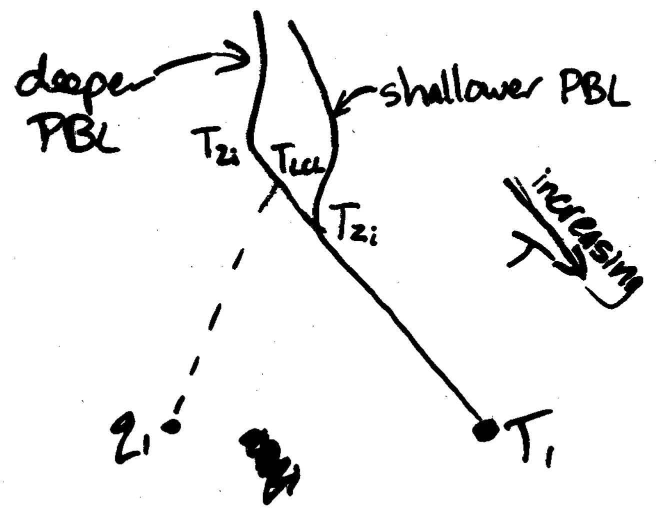

stability depends on difference between T_{zi} and T_{LCL}

profile will be more stable if $T_{zi} >> T_{LCL}$

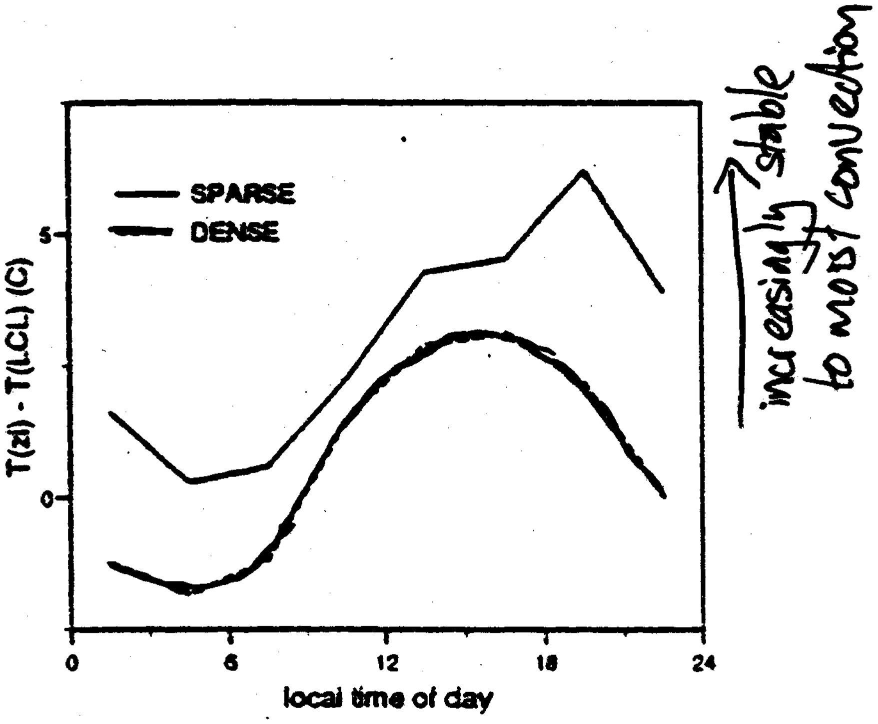

SPARSE is more stable than DENSE on average ∴ expect less frequent convection

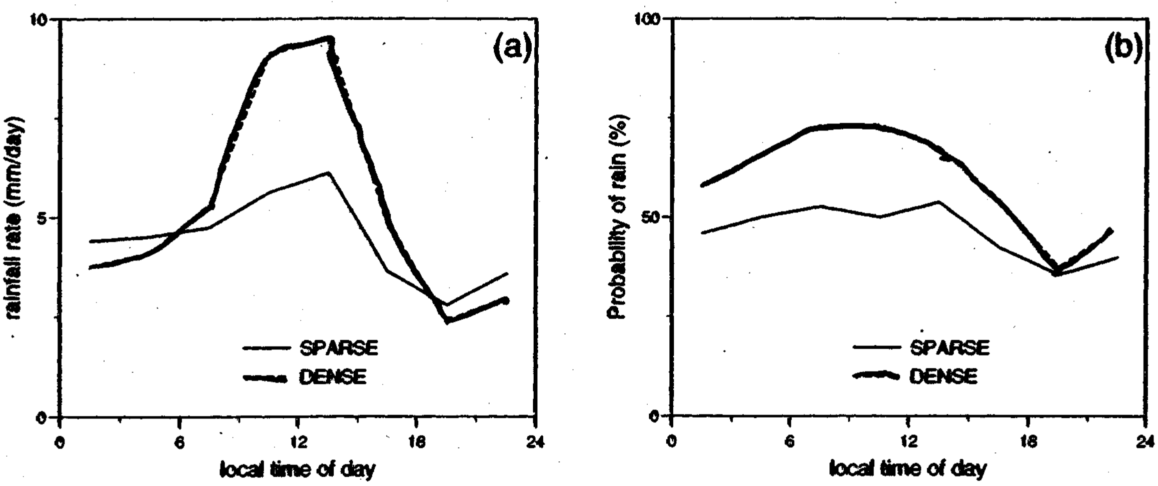

Figure 5. Mean July to September diurnal cycles averaged between 15°W–11.25°E, 12.5–15°N: (a) rainfall rate (mm day^{-1}), (b) probability of rainfall during a three-hour period (%).

Improved surface parameters
dampen (erroneous) diurnal signal

- convection less frequent
- 20% increase in sw radiation reaching the surface

Rainfall Spectra

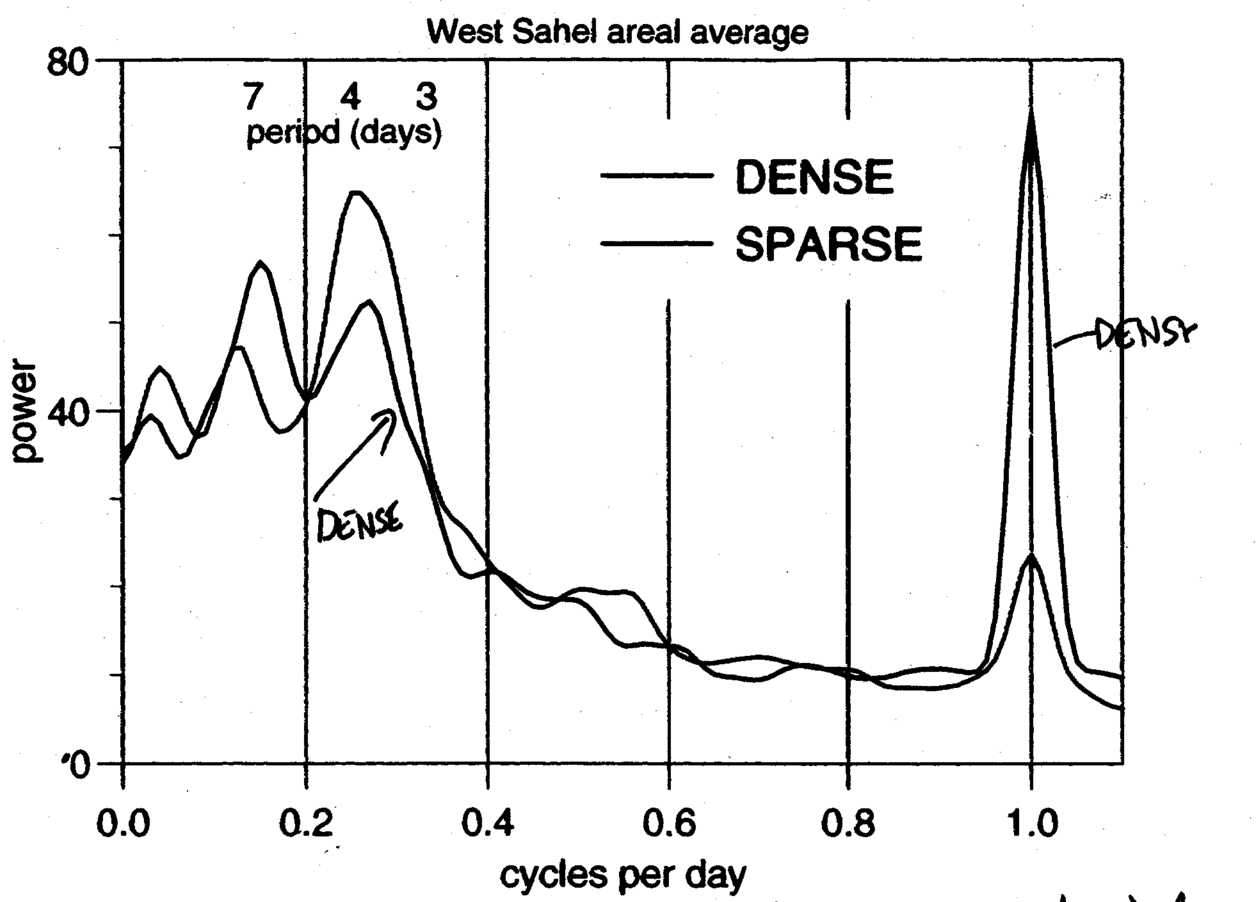

decrease in peak at 1 day & increase at 4 days

700 hPa Meridional Wind Spectra

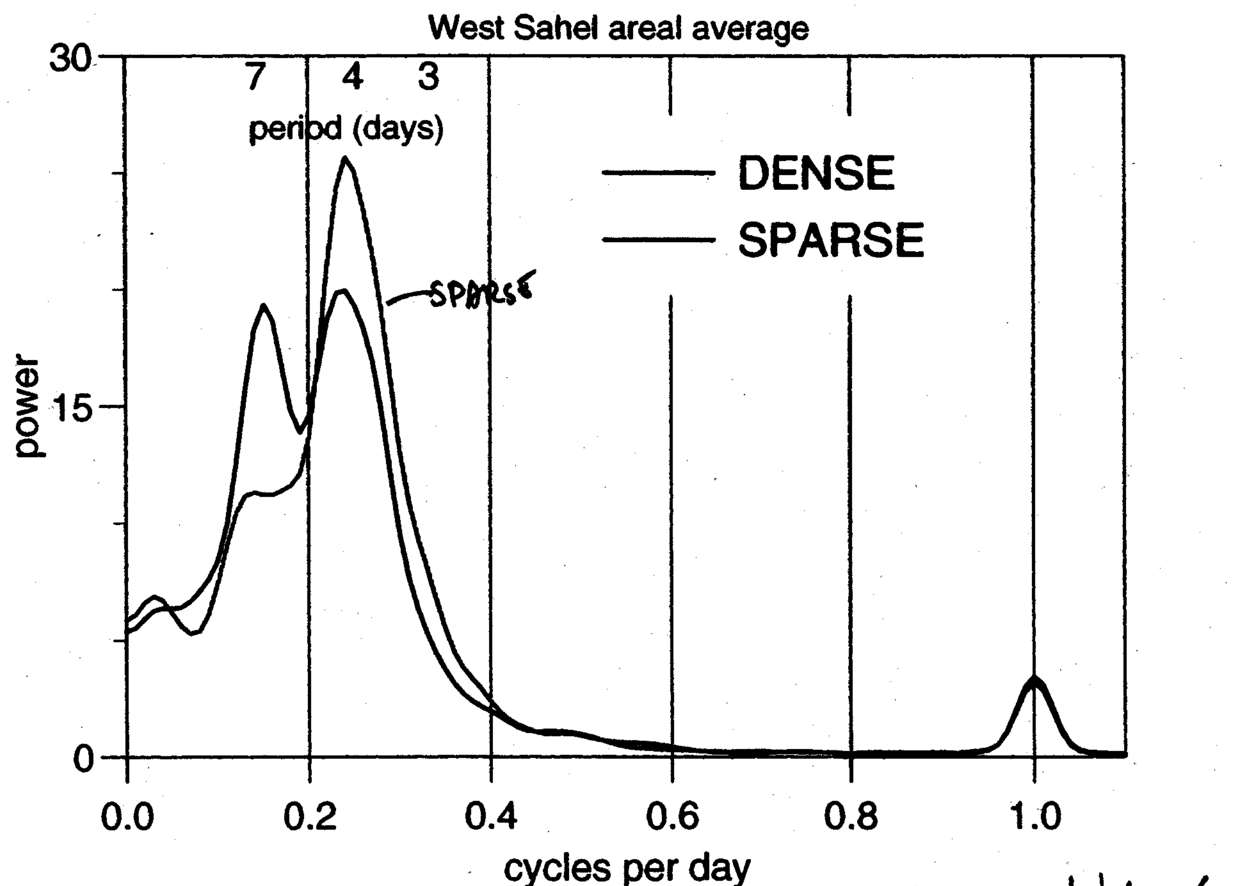

also SPARSE has more synoptic variability (see later)

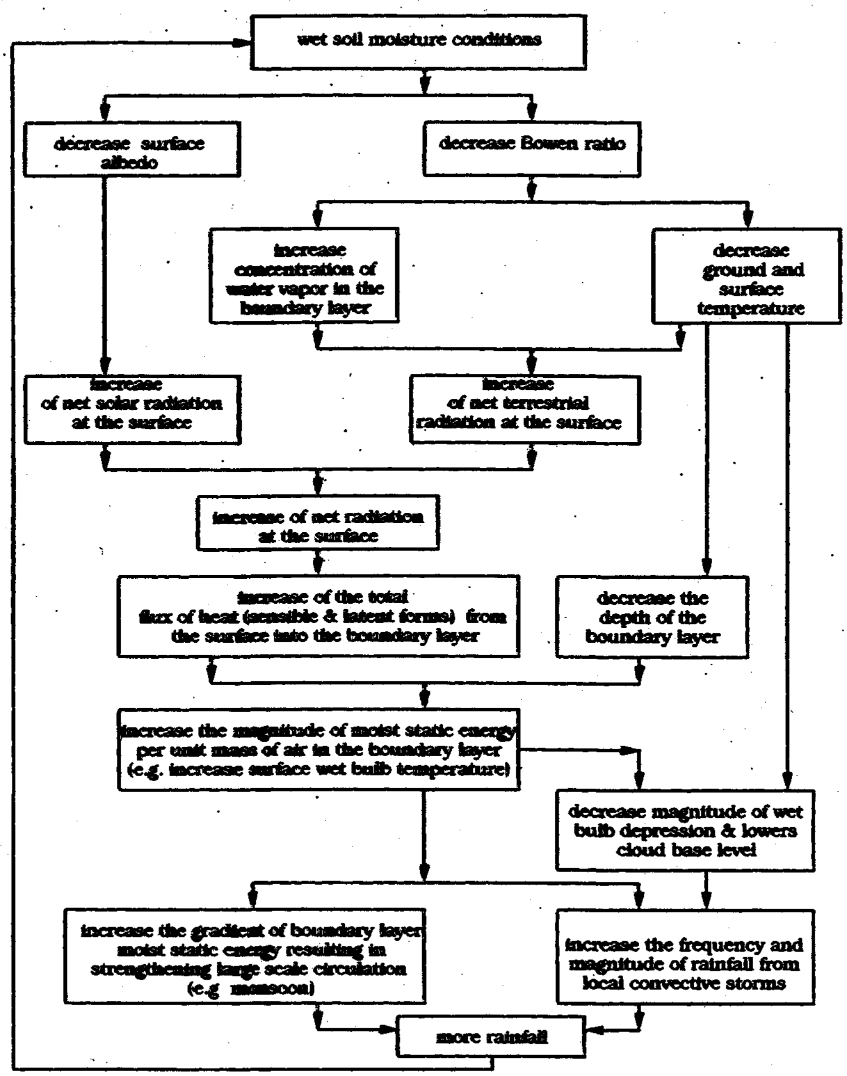

Figure 2. The proposed hypothesis for relating soil moisture conditions and subsequent rainfall processes.

cal Research [*Sellers et al.*, 1992]) and are presented here to support the proposed hypothesis. Section 4 describes the relationship between soil moisture and boundary layer energy. Section 5 covers the role of clouds in the surface radiation processes. Section 6 includes a discussion and conclusions.

2. Theory

Here we propose a hypothesis that describes the role of soil moisture in land-atmosphere interactions. In particular, we suggest that wet soil moisture conditions enhance the following related variables: net surface radiation, total heat flux from the surface into the atmosphere, and moist static energy in the atmospheric boundary layer. The latter can be quantified using several variables including wet bulb potential temperature and equivalent potential temperature. These two variables are important for the energetics and dynamics of local convective storms [*Williams and Renno*, 1993; *Eltahir and Pal*, 1996; *Zawadzki and Ro*, 1978; *Zawadzki et al.*, 1981] as well as the dynamics of large-scale atmospheric circulations in the tropics [*Emanuel et al.*, 1994; *Eltahir*, 1996; *Eltahir and Gong*, 1996]. The proposed pathways for relating soil moisture conditions and subsequent rainfall are described in Figure 2. We hypothesize that Figure 2 describes the dominant pathways for relating soil moisture and subsequent rainfall. However, this figure is not designed to describe all possible interactions. The proposed hypothesis is based on considerations of the following: (1) the relationship between soil moisture conditions and two basic properties of the land-surface, albedo and Bowen ratio; (2) the surface radiation balance; (3) the energy balance at the land-atmosphere boundary; (4) the energy balance of the atmospheric boundary layer; and (5) the thermodynamic and dynamic processes that relate boundary layer conditions and subsequent rainfall.

2.1. Basic Properties of the Land Surface: The Relationship Between Soil Moisture Conditions, Surface Albedo, and Bowen Ratio

The role of soil moisture conditions in regulating surface albedo and Bowen ratio is the fundamental basis of the proposed hypothesis. Basic radiation physics suggests that water absorbs significantly more solar radiation than dry soil. As a result, absorption of solar radiation increases with the relative fraction of water in any mixture of soil and water. Several observations confirm these theoretical arguments. *Bowers and Hanks* [1965] and *Bowker et al.* [1985] studied the spectral reflectance of soil surfaces and confirmed that at all wave lengths of solar radiation, reflectance decreases with the level

Observational evidence of soil moisture rainfall feedback

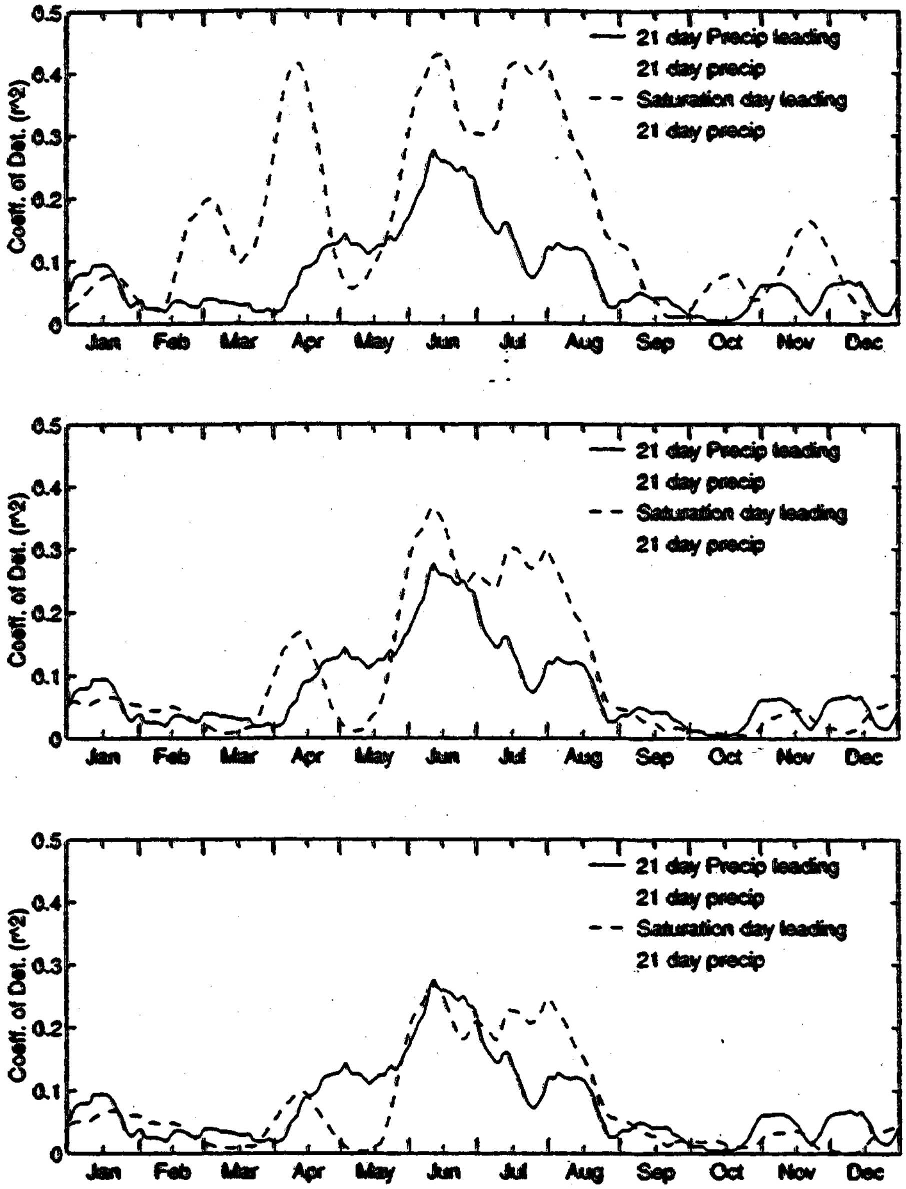

Figure 7. Comparison of smoothed lines of the correlation between adjacent precipitation windows (top) top 10 cm, (middle) top 50 cm, and (bottom) top 90 cm) (solid line, from Figure 5) and of the correlation between soil saturation and subsequent precipitation (dashed line, from Figure 4).

variability will go down as the inverse of the length of the averaging window. All Figures 4a–4c show the daily r^2 is stronger during the summer than the rest of the year, though there is a local peak during April, as well. At the shallower depths the linear correlation stays above the 10% level of significance line from the end of May to early August and for much of April. During the rest of the year the correlation between soil moisture and subsequent precipitation is not significant.

We find three possible explanations for these results showing that there is a significant linear relation between soil saturation and subsequent precipitation conditions during this summer period. First, it is possible that the relationship is due to a persistent large-scale atmospheric forcing that sustains or enhances a persistence in rainfall between adjacent time periods, and through the correlation between concurrent rainfall and soil saturation, results in the observed correlation between soil saturation and subsequent rainfall. Second, the correlation could be a reflection of a feedback process in which initial soil moisture affects rainfall, which then affects soil moisture, etc. Finally, we must consider a combination of these two mechanisms.

If large-scale atmospheric processes drive the system at hand, persistence in atmospheric conditions would first be reflected in rainfall persistence, as shown in Figure 5. Here persistence in rainfall is measured by the correlation between the total precipitation in adjacent 21-day windows. Figure 6 then shows the correlation between a 21-day rainfall window and soil saturation at the end of the window. If precipitation forces soil saturation at the end of a given window (Figure 6), and if precipitation is also linearly correlated with precipitation in the next time window (Figure 5), soil saturation may, merely as a direct consequence of this rainfall forcing, also be significantly correlated with subsequent precipitation (Figure 4). In this case, we would expect the rainfall persistence to be greater

II Raintall Persistence HAPEX-Sahel

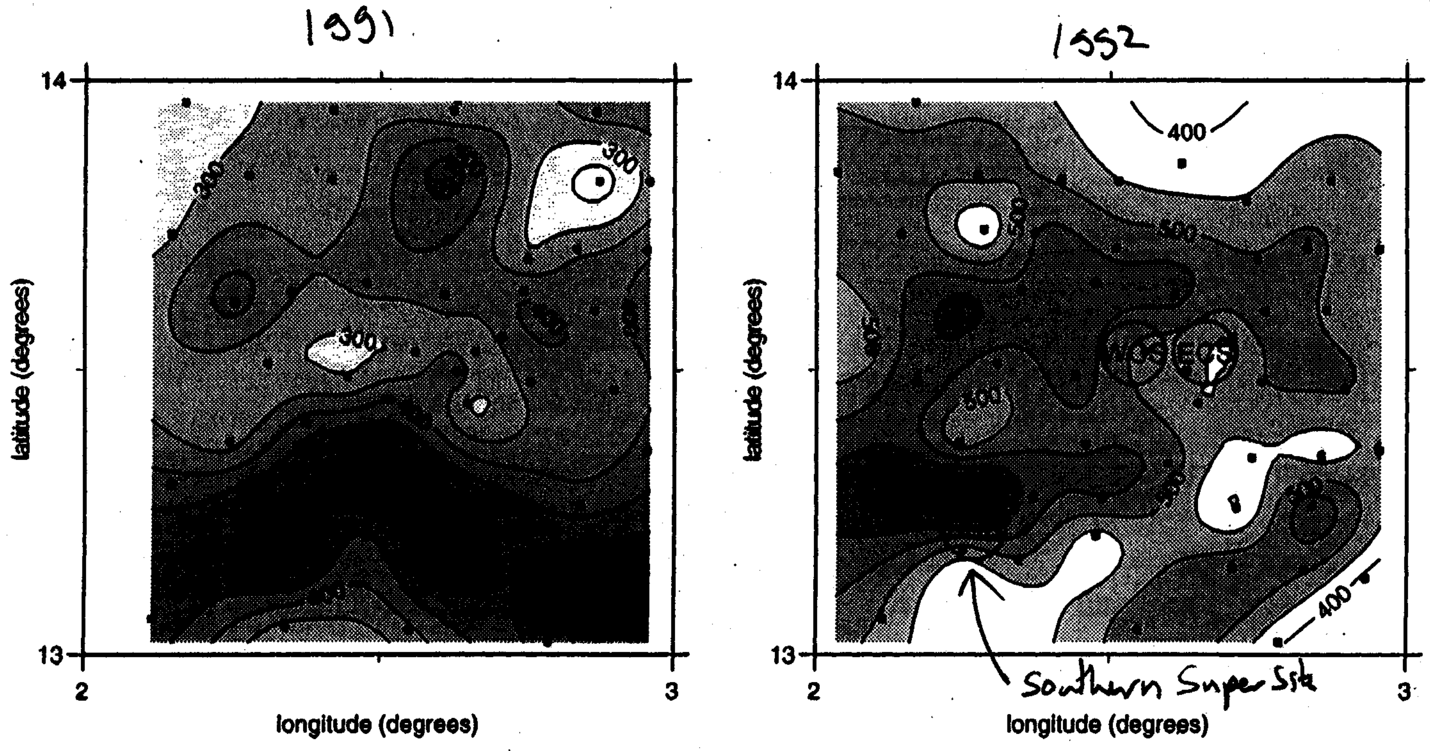

(a) (b)

seasonal raintall totals

references: Taylor et al 1997
Taylor + Lebel 1998
Taylor 2000

Spatial variability of rainfall - series of storms

Southern Super Site

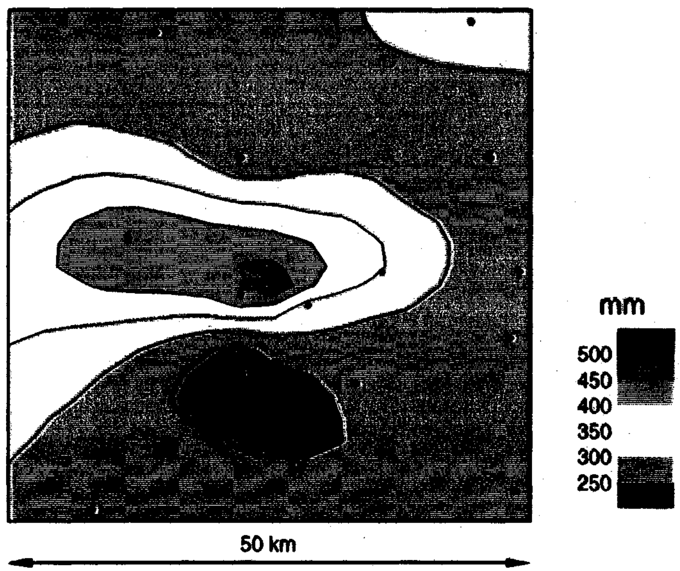

July 31 - September 18 1992

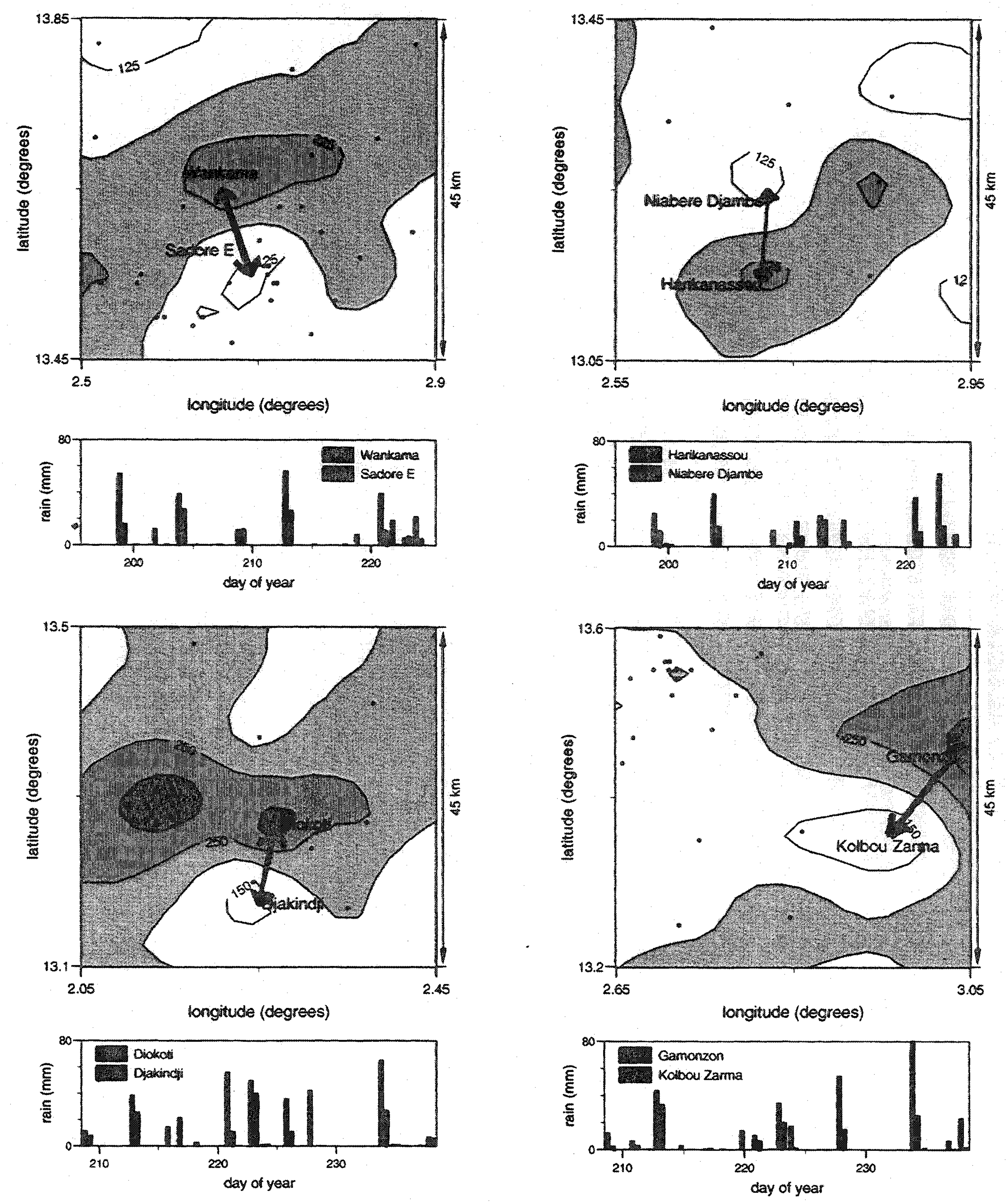

Differences accumulate over several events.

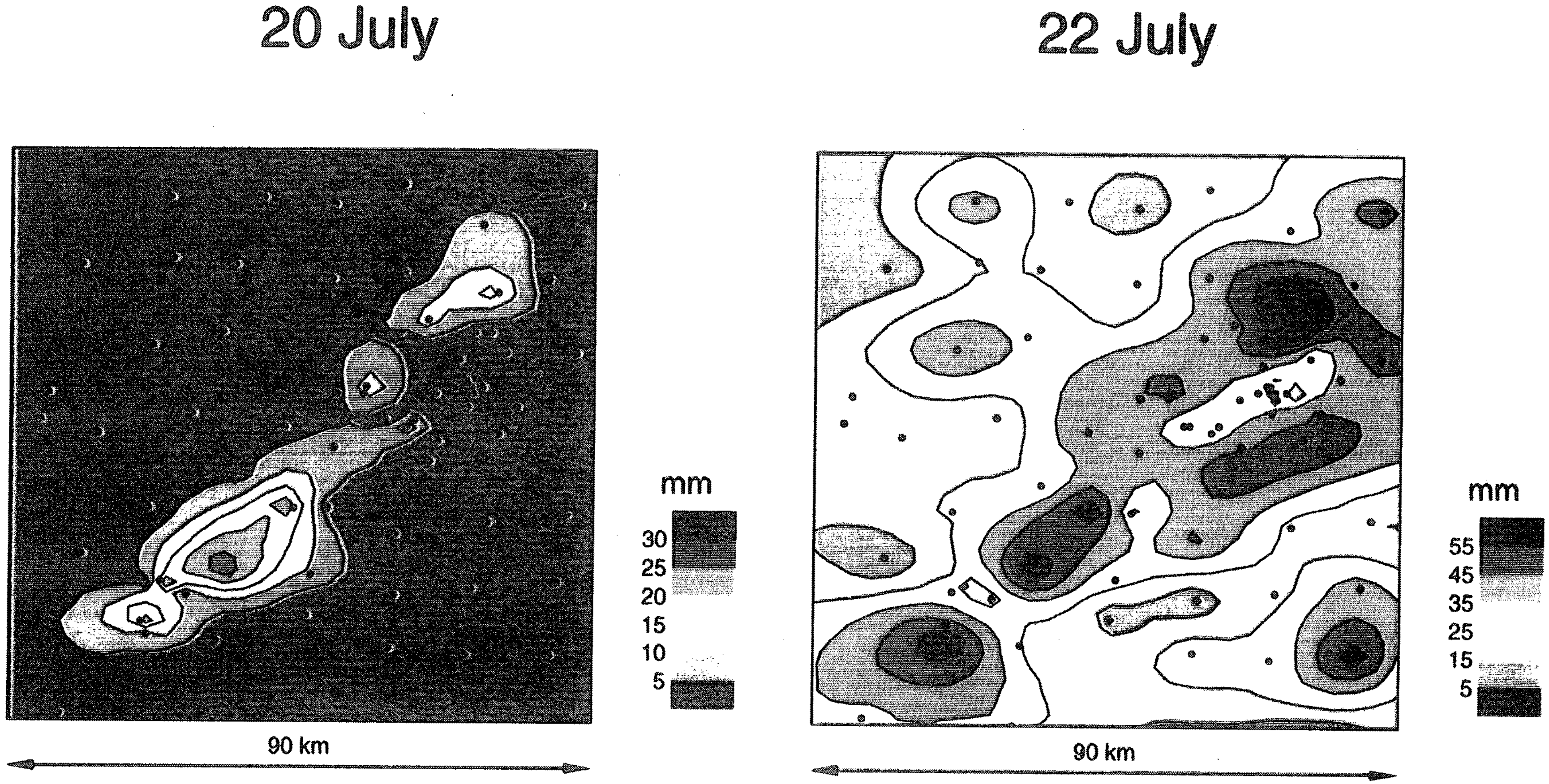

- tendency of rain within squall lines to be heavier in locations that have been recently wetted
- suggests a positive feedback between soil moisture and rainfall at scales of 10-15 km

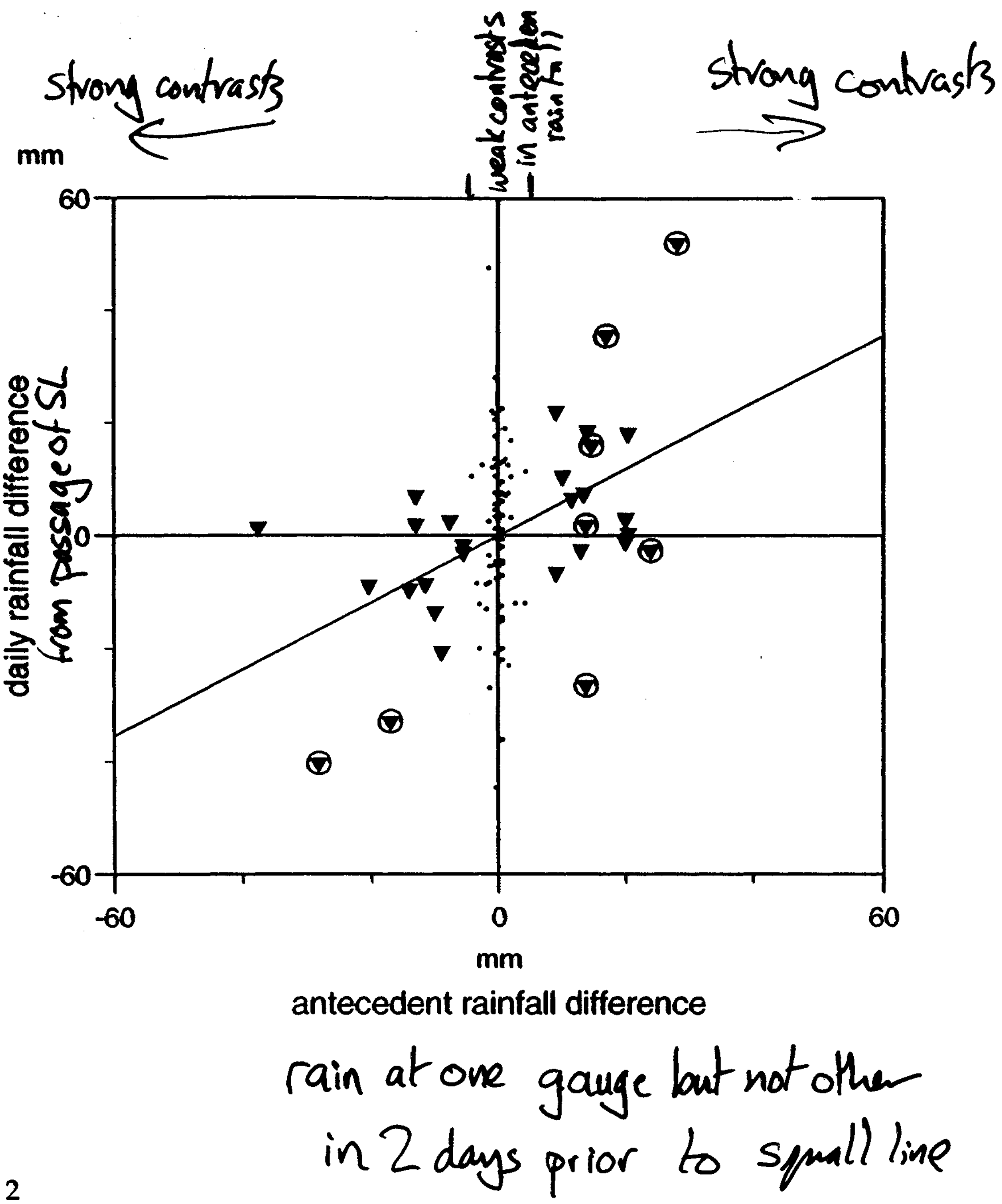
strong contrasts
weak contrasts in antecedent rainfall
strong contrasts
mm
60
0
-60
-60
0
60
mm
daily rainfall difference
from passage of SL
antecedent rainfall difference
rain at one gauge but not other in 2 days prior to squall line

Fig. 2

similar pattern
looking at rain in previous 10 days

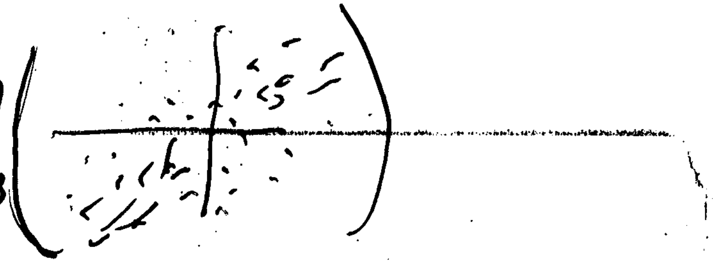

(b)

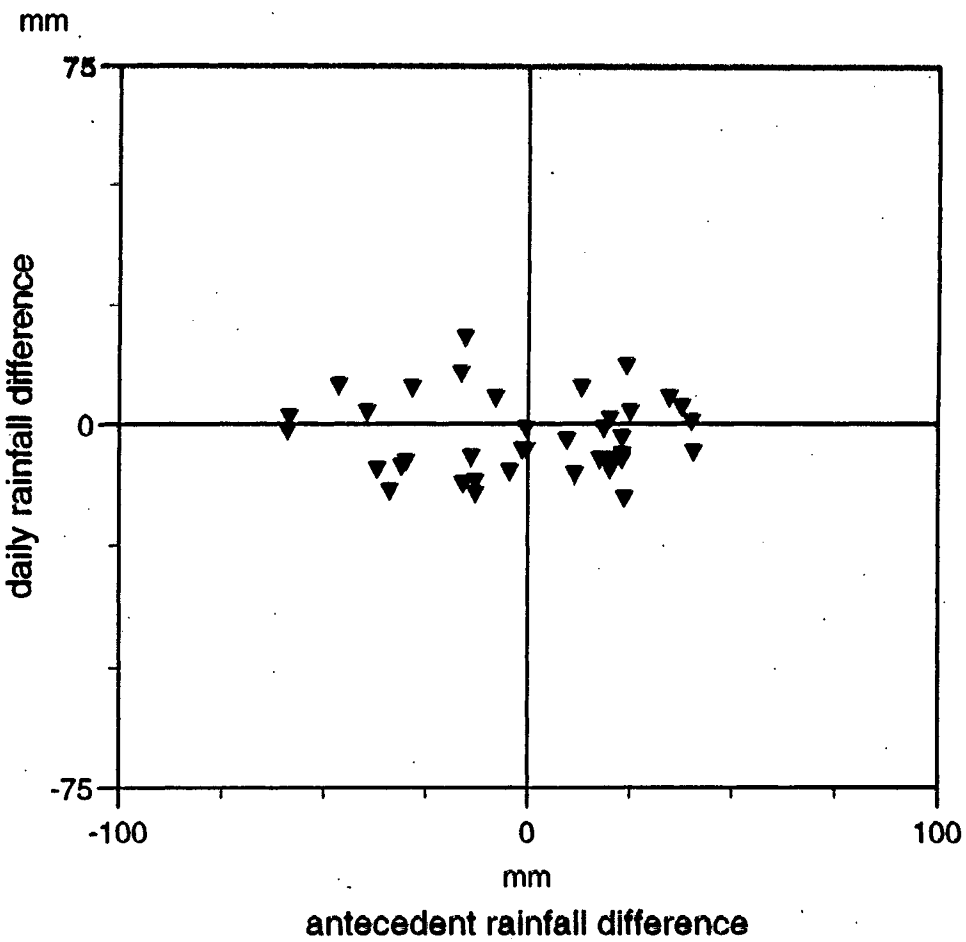

but not when it's rained at both gauges within previous 24 hours

The Southern Super Site in HAPEX-Sahel

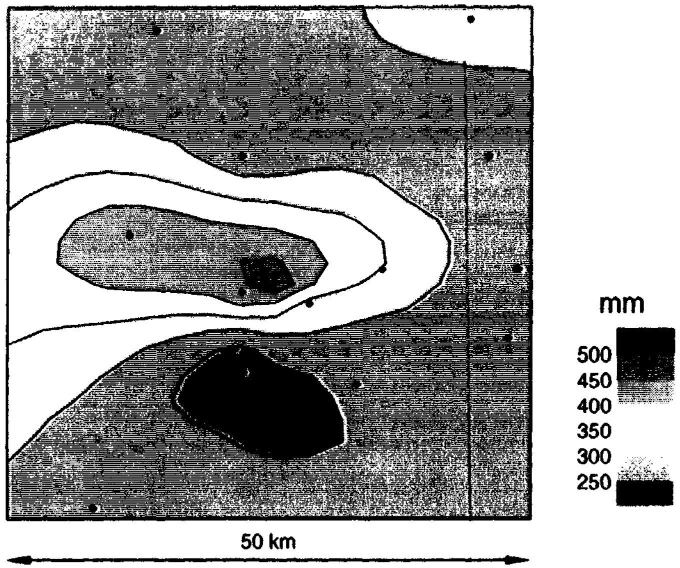

Contrast of 284 mm
over 9 km
during 1992

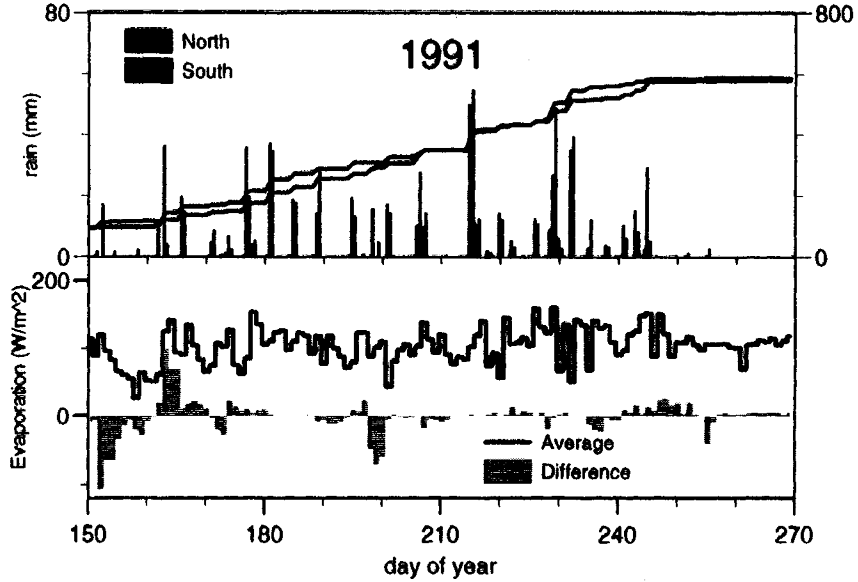

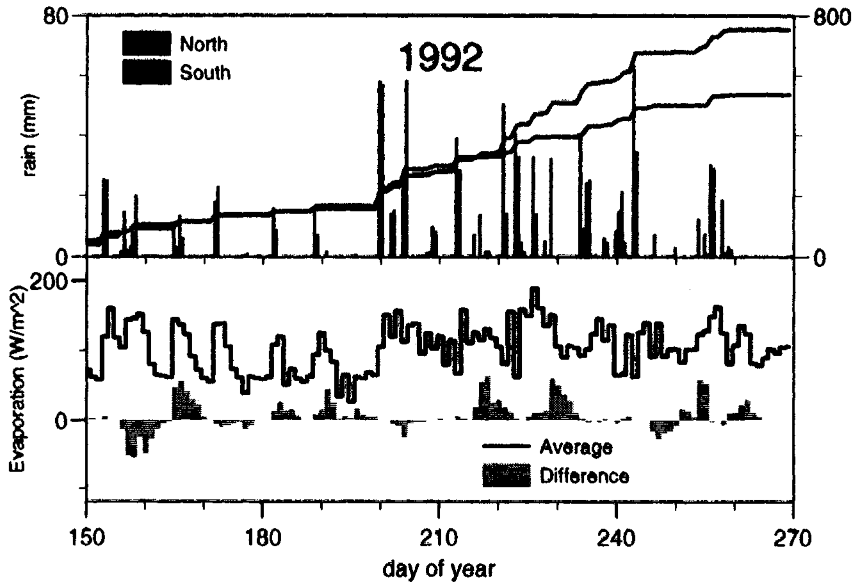

aircraft observations see Taylor et al 199?

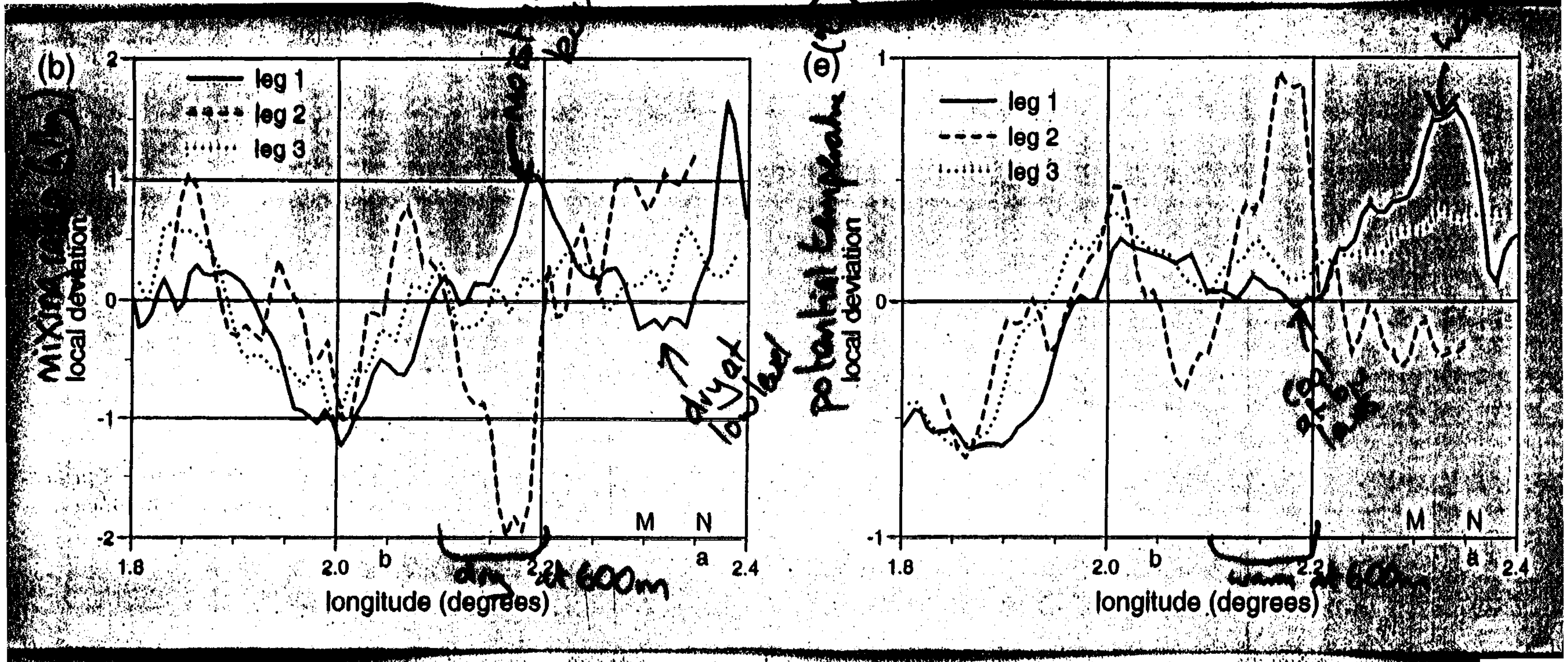

leg 1 50m height

leg 2 600m (close to PBL top)

leg 3 300m

between 11 ...

local ...

light wind...

aircraft show anti-correlated T and q on scales ~10 km weather station data

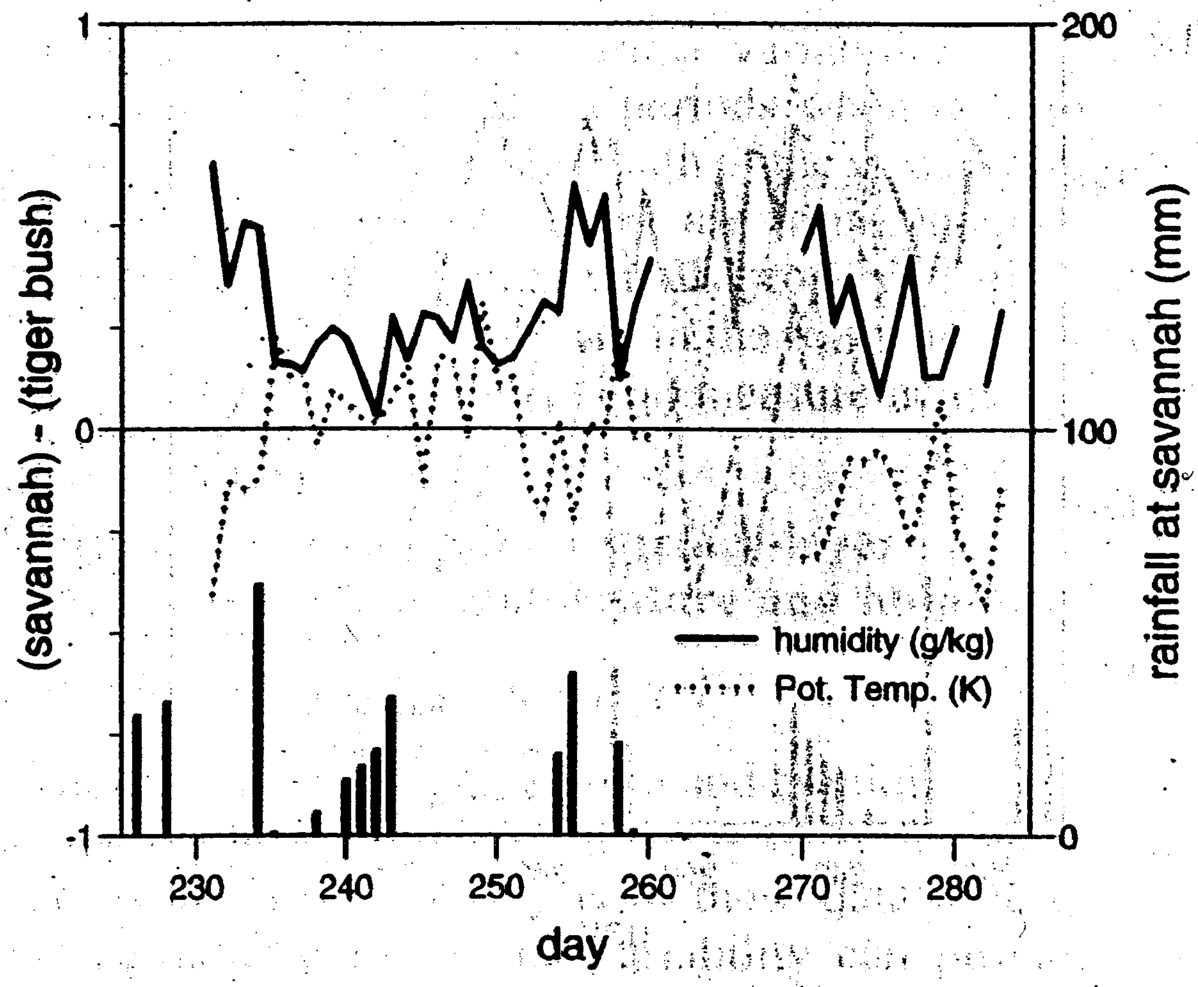

FIG. 7. Differences at 9.5 m in specific humidity (g kg^{-1}) and potential temperature (K) between the savannah and tiger bush sites, averaged over a day. Daily rainfall (mm) at the savannah site is also

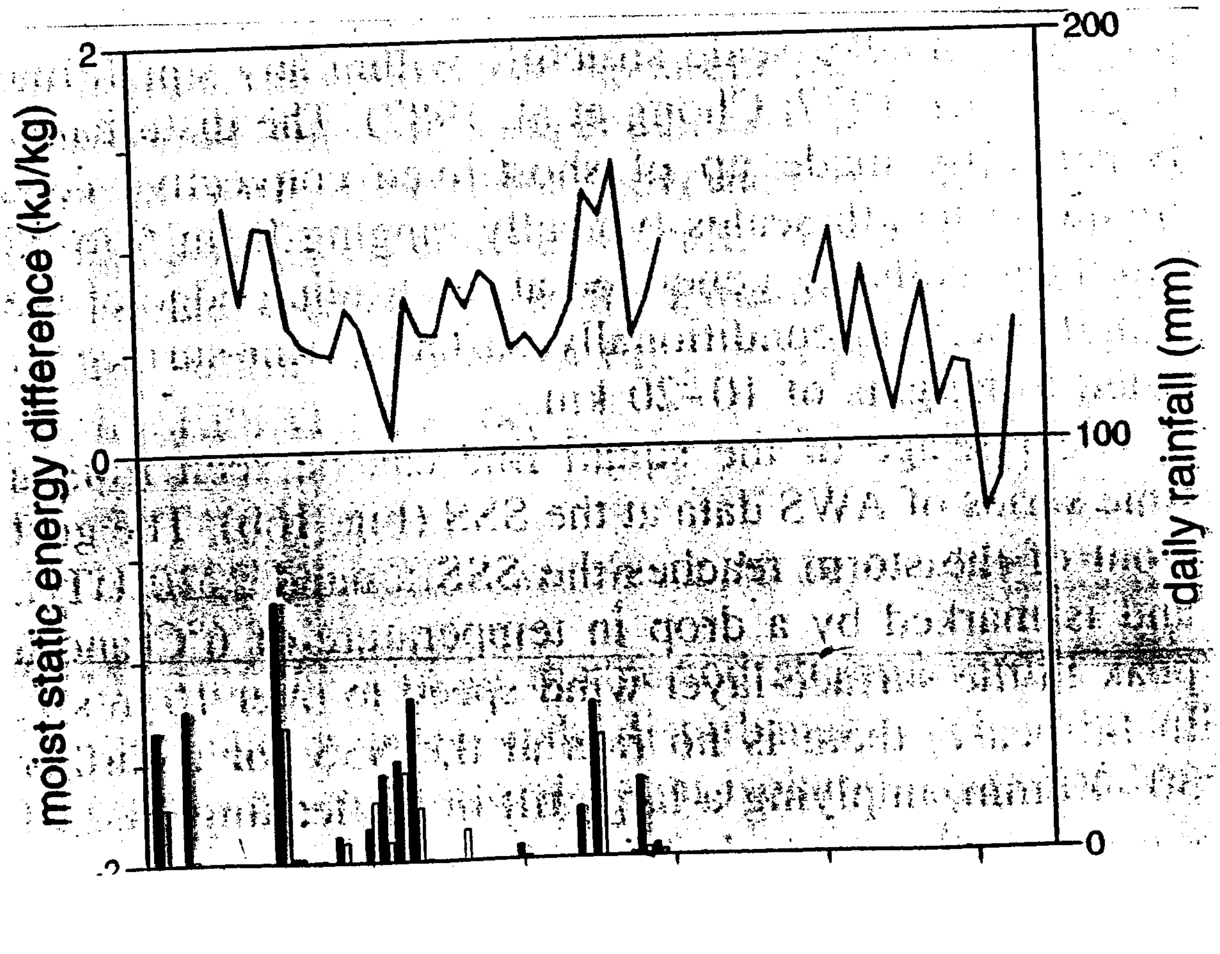

Impact on planetary boundary layer

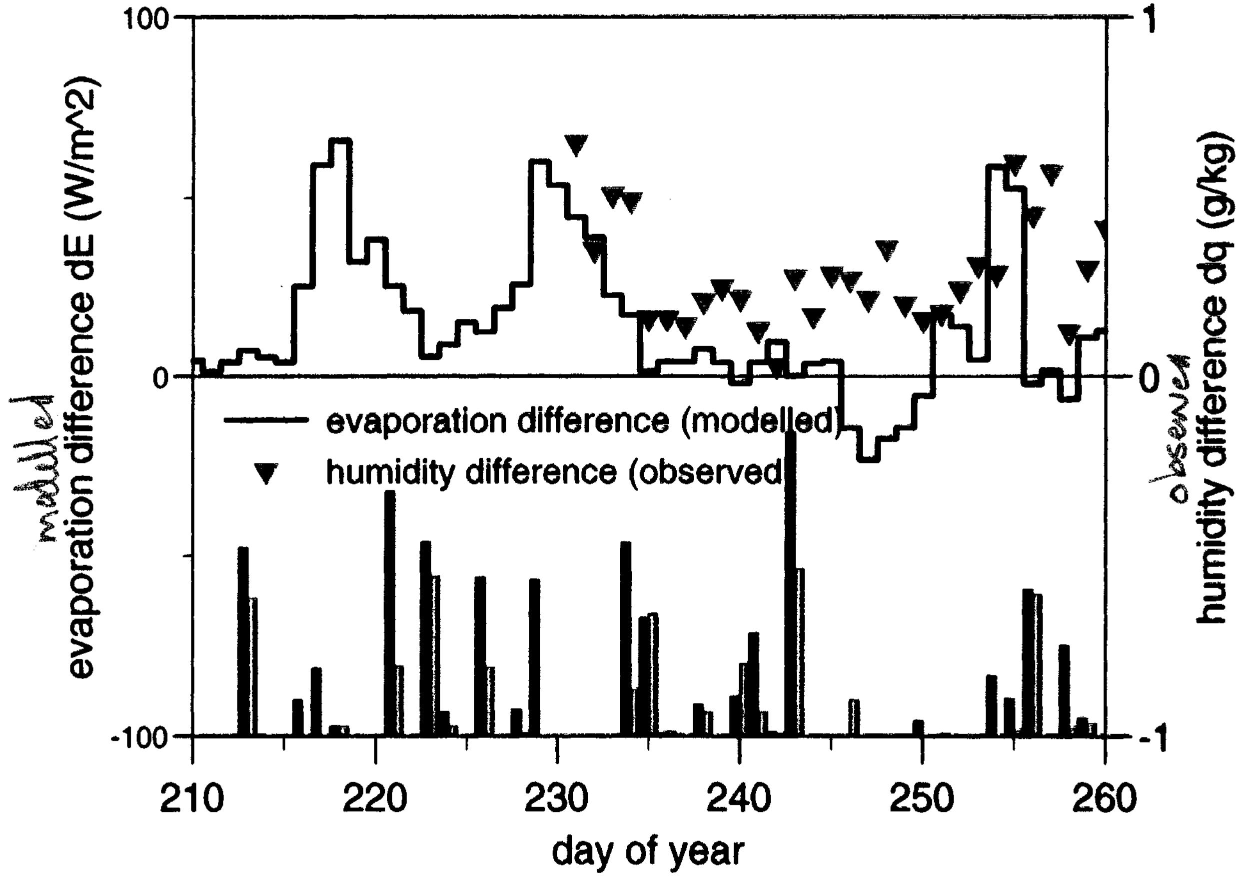

2D modelling using RAMS in cloud resolving mode
$\Delta x = 1km$
convection resolved

Rainfall from a squall line crossing wet and dry patches

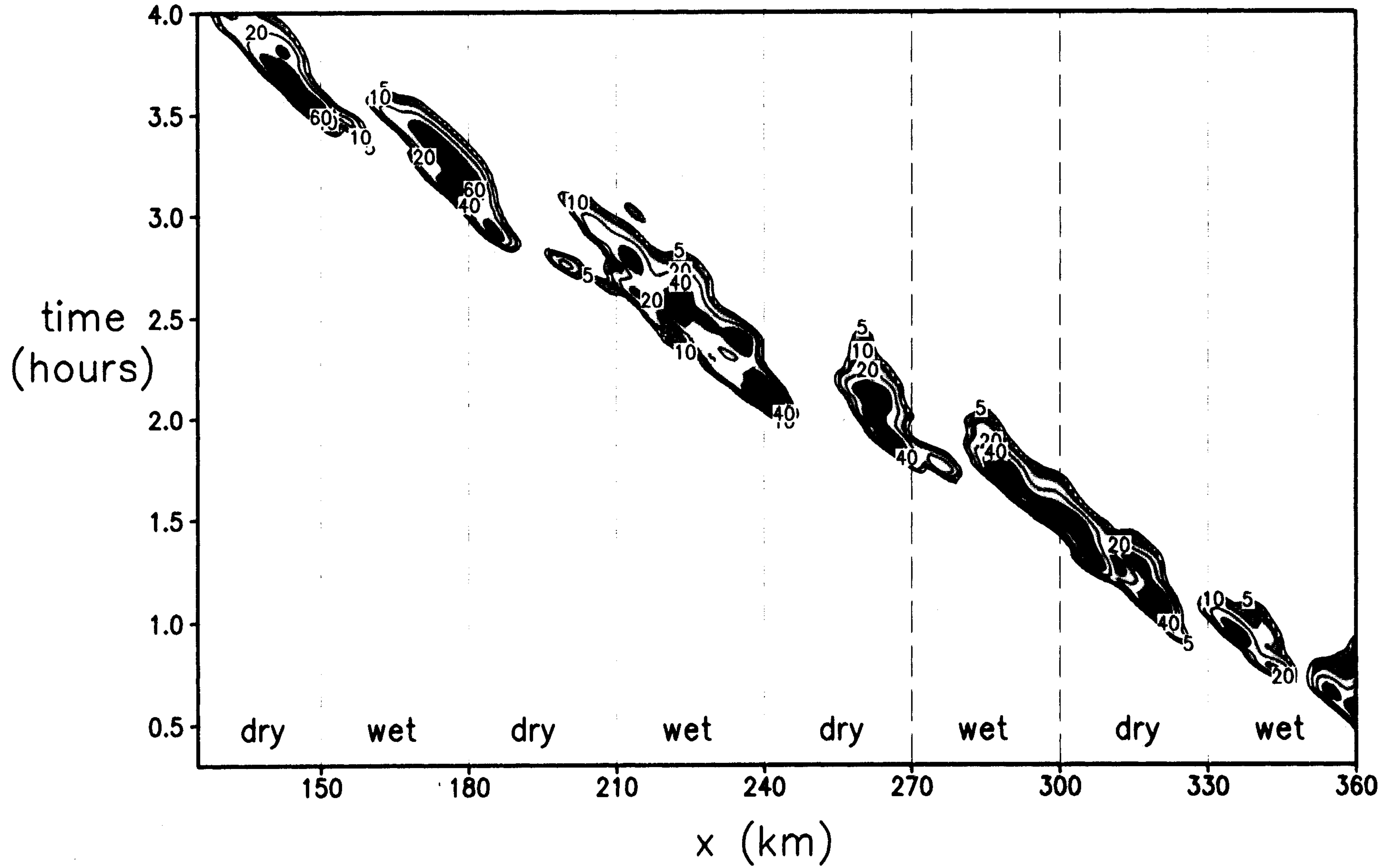

Initial results (2-D case)

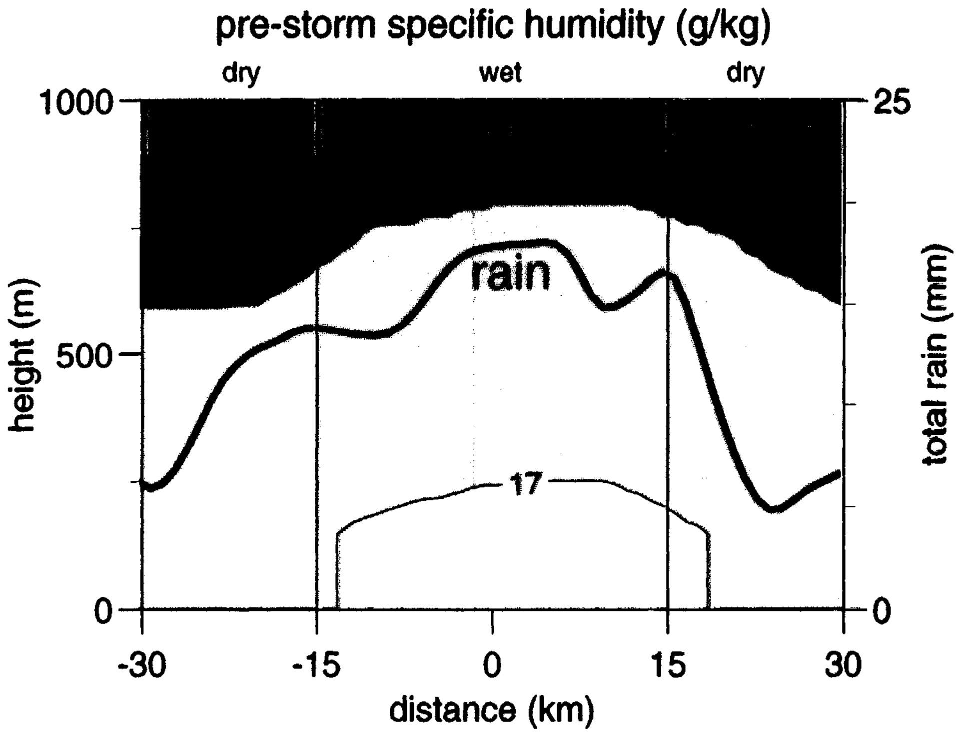

Soil moisture profiles:

Wet patch:
10mm rain 6 hours prior to storm

Dry patch:
no rain for 4 days

Average rainfall: wet patch 15.8mm
dry patch 9.3mm

III Synoptic Variability - African Easterly Waves

Land Surface Impacts on Rainfall Systems in a GCM

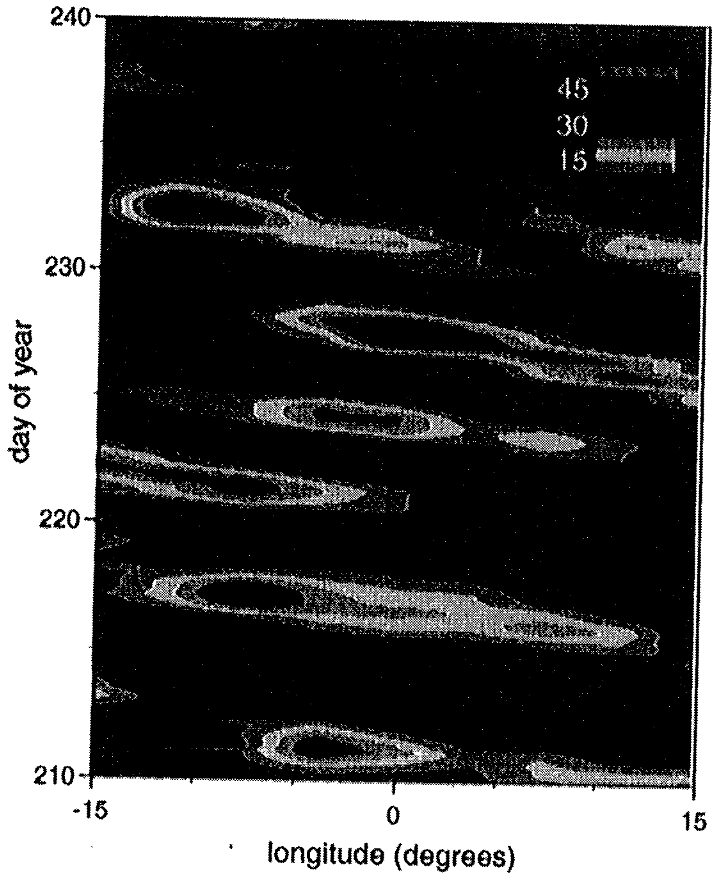

UKMO/Hadley Centre GCM

- rainfall dominated by travelling disturbances
- squall lines not represented
- rain modulated by African Easterly Wave activity

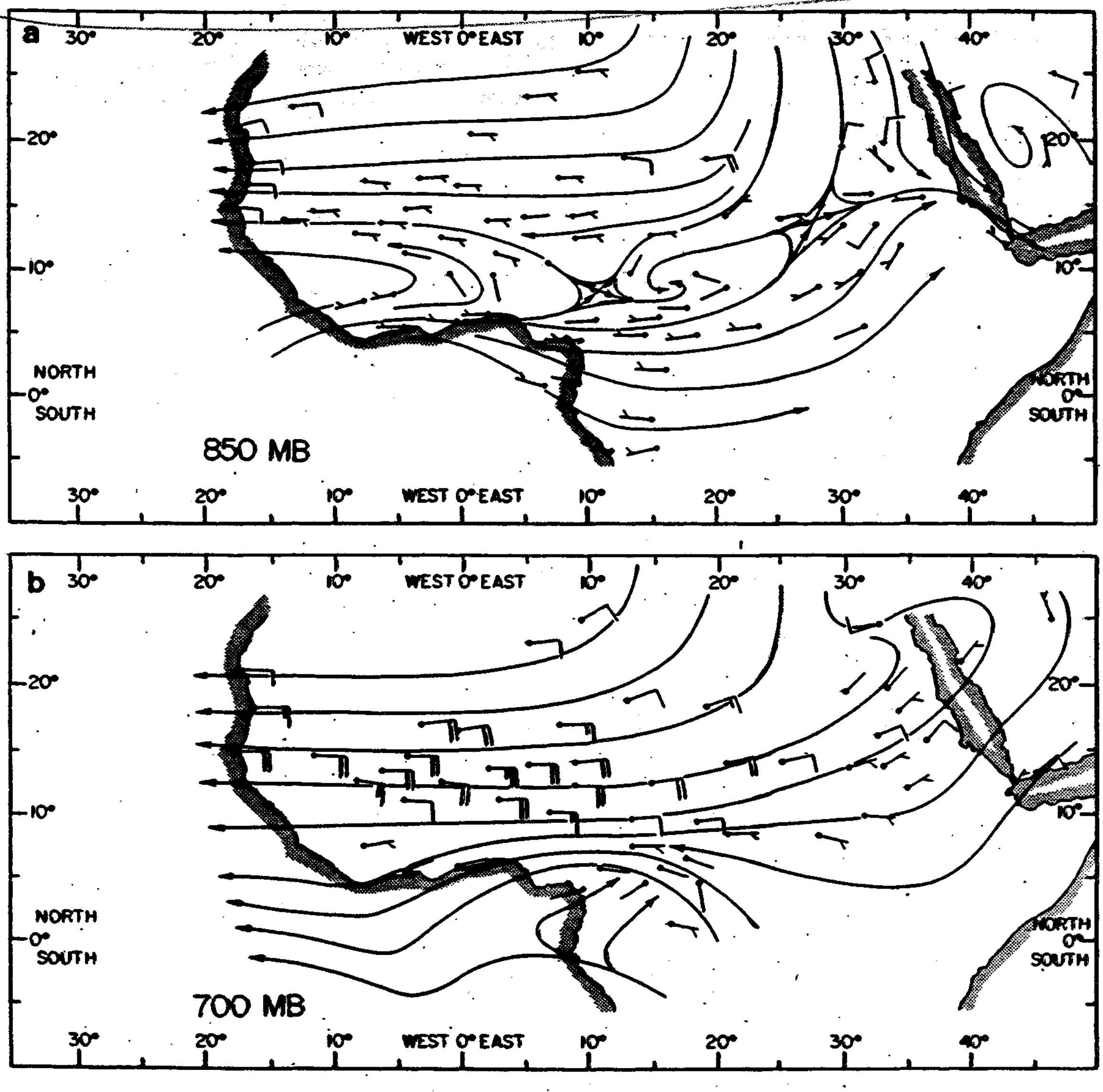

FIG. 2. Mean wind fields for the period 23 August–19 September 1974: (a) 850 mb (b) 700 mb. Half barb indicates 2.5 m s^{-1}, a full barb 5 m s^{-1}.

African Easterly Jet during the GATE experiment

The results of the spectral analysis at 850 mb are displayed in Fig. 3. The isopleths depict the amplitude of the meridional wind component in the frequency band 0.2–0.4 cpd (cycles per day) (periods between 2.5 and 5 days). The amplitude was obtained by taking the square root of twice the power (variance) in that frequency band. The most prominent feature of the diagram is the dumbbell-shaped area of large amplitude with centers of maximum amplitude located near the Greenwich meridian and the coast. From the shape of the pattern we conclude that the disturbances experienced their main growth between 10°E and 0°, weakened somewhat between 0° and 10°W, and then reintensified near the coast. In conformity with the description given in pre-GATE studies employing synoptic and satellite data (Carlson, 1969b), the disturbances diminished rapidly in strength after leaving the coastal waters.

The analysis has been extended to the GATE ship array in order to show how the amplitudes in the A/B-scale network, where the disturbances have been thoroughly documented (Thompson *et al.*, 1979), compare with those over the upstream continental area. Spectra for the ships and the two stations in the Cape Verde Islands (locations shown in Fig. 1) are based on 21 days of data (30 August–19 September, inclusive) rather than on the 28 days available for land stations. Because of the slight difference in periods, the isopleths do not exactly mesh at the coastline. Calculations of the land spectra based on the shorter 21-day period revealed only slight differences from those based on the full period. The

The geographical distribution of the amplitude in the 2.5–5 day band and character of the spectral peaks for the meridional wind component at 700 mb are shown in Fig. 7. The main features of the amplitude distribution resemble those at 850 mb except for a general southward shift of the regions of larger amplitude. The major increase in amplitude again

The direction of phase propagation and coherence squares at 700 mb are shown in Fig. 8. Along the line extending from Dakar (61641) to Djibouti (63125) and Aden (40597) the phase propagation is everywhere westward or neutral and coherence squares remain large as far east as 20°E. Consequently, it seems worthwhile to seek further evidence

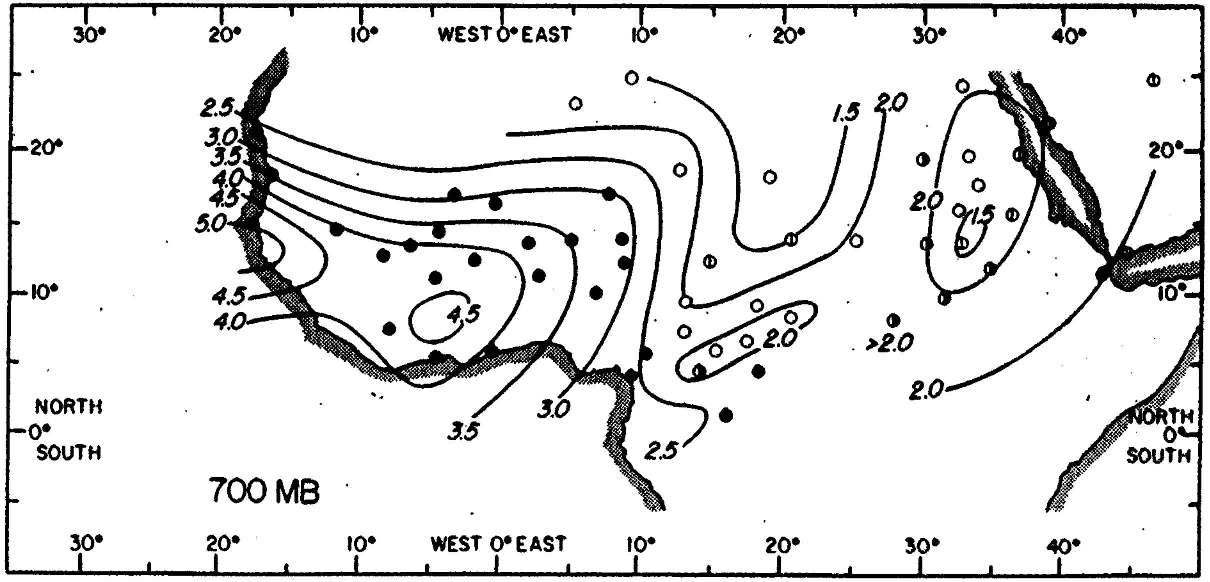

FIG. 7. Amplitude of meridional wind oscillation in 0.2–0.4 cpd frequency band at 700 mb. See Fig. 3 for further explanation.

(location of wave activity)
Albignat + Reed

as large as in the western
indicated with a wavelengt
speed of 8.8 m s⁻¹. These v
eters are sufficiently close t
to raise the possibility of a
as the southern Arabian Pe
The studies of Burpee (1
(1977) suggest that both ba
energy conversions associat
the mid-troposphere jet st
growth of African waves. Th
is proportional to the prod
eddy flux of zonal momentum
of the mean zonal wind (∂
momentum away from the j
momentum toward the core i
the expense of the mean zon
The eddy flux at 700 mb a
cospectra of the meridional a
nents is shown in Fig. 10a. A
location of the jet axis taken
parent that the flux reverses si
length of the jet axis, signif
flow of easterly momentum a
of wave energy nearly everyw
est fluxes occur west of 10°E w
the wave amplitudes are large
mum is present over southern S
of a weak wave signal was f

West African Circulation

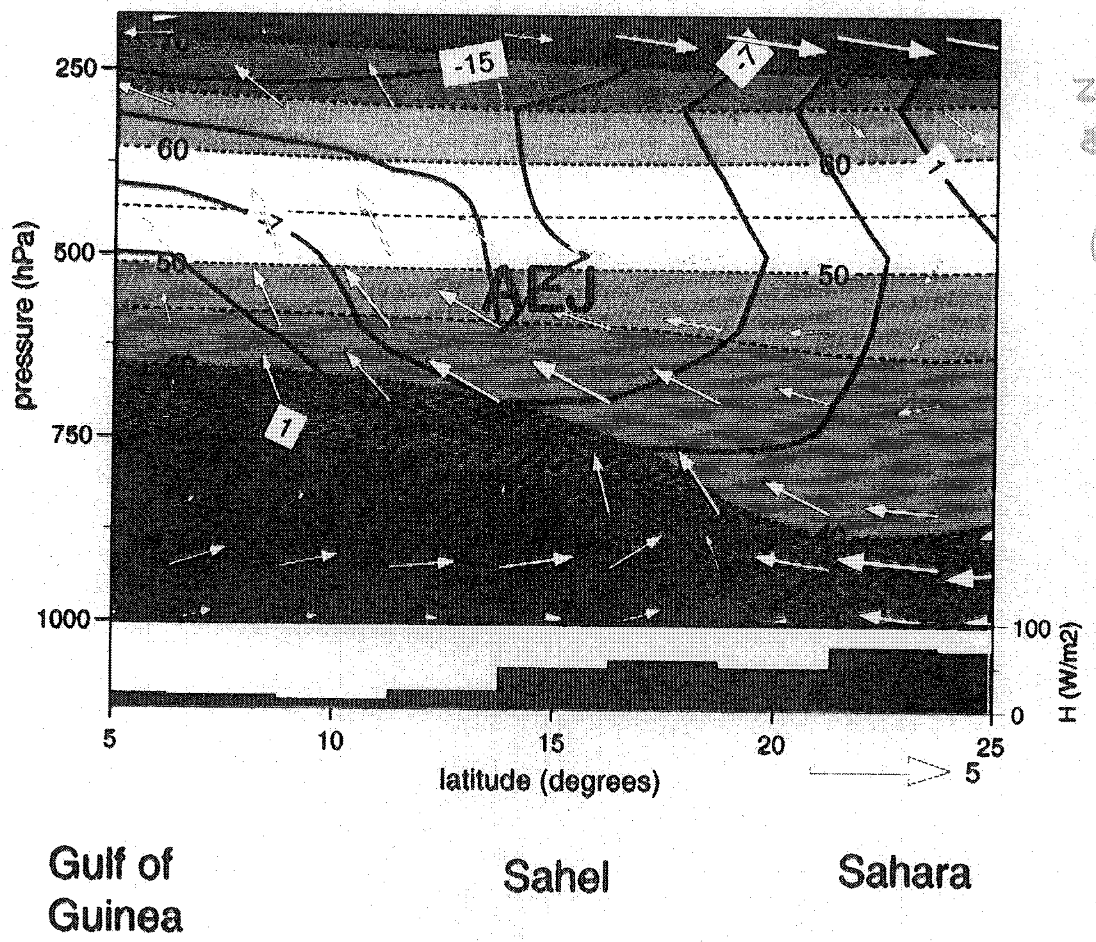

zonal mean from Unified Model
(see Taylor + Clark 2001)

Constructing a composite African Easterly Wave

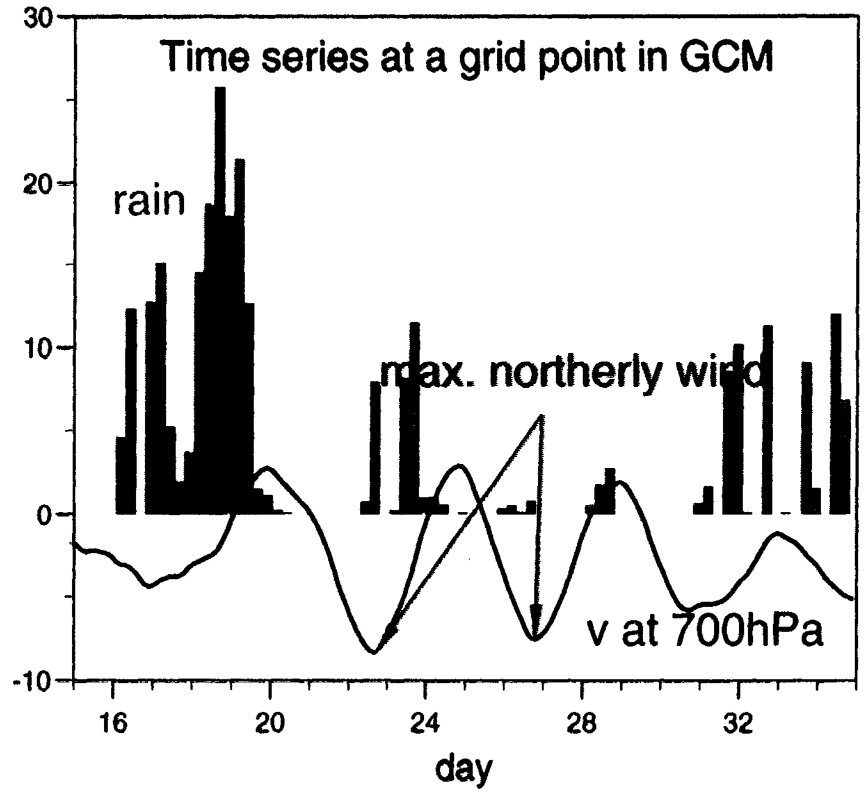

Composite Wave from GCM

- based on time of passage of maximum northerly wind at 700 hPa

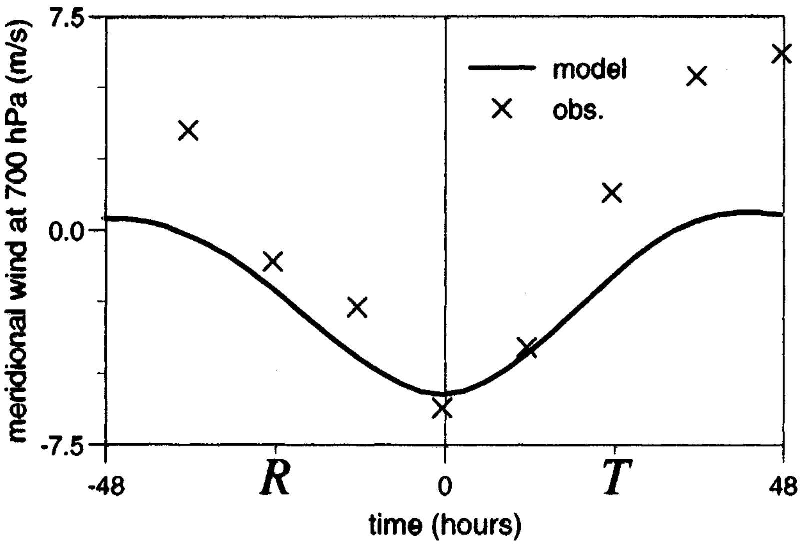

comparable with GATE composite (Reed et al 1977)

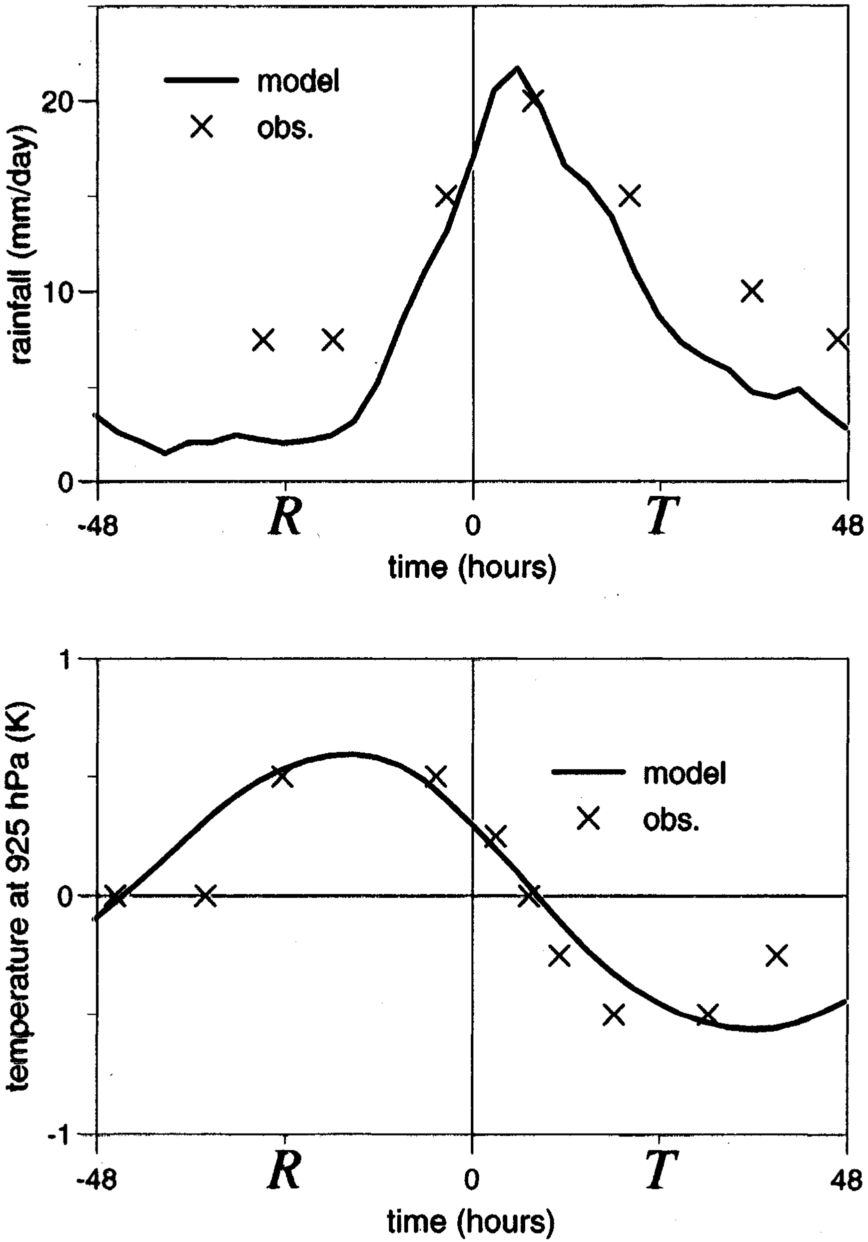

model compares
well with
observation

Surface flux variability across wave

composite ... in GCM

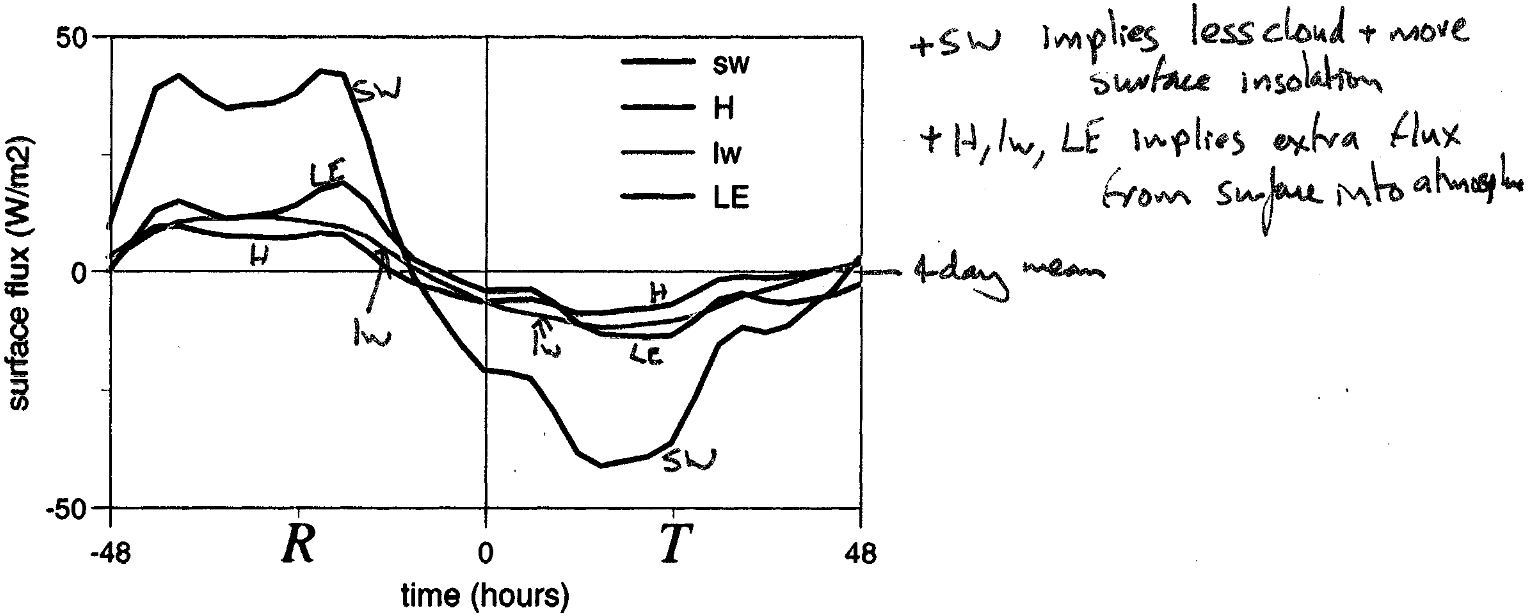

large daily variations in land surface fluxes due to

- surface moisture availability
- cloudiness

PBL Budget Calculations

Estimate PBL heating and moistening rates due to surface flux variability

Potential Temperature

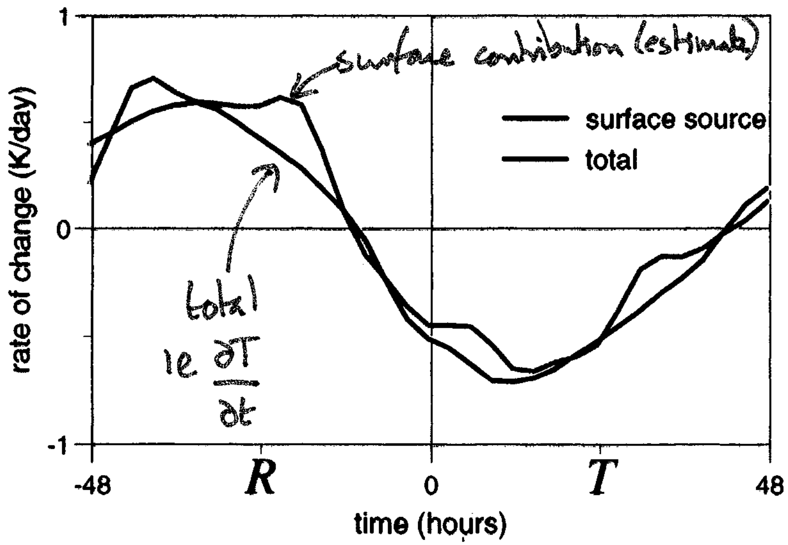

Equivalent Potential Temperature

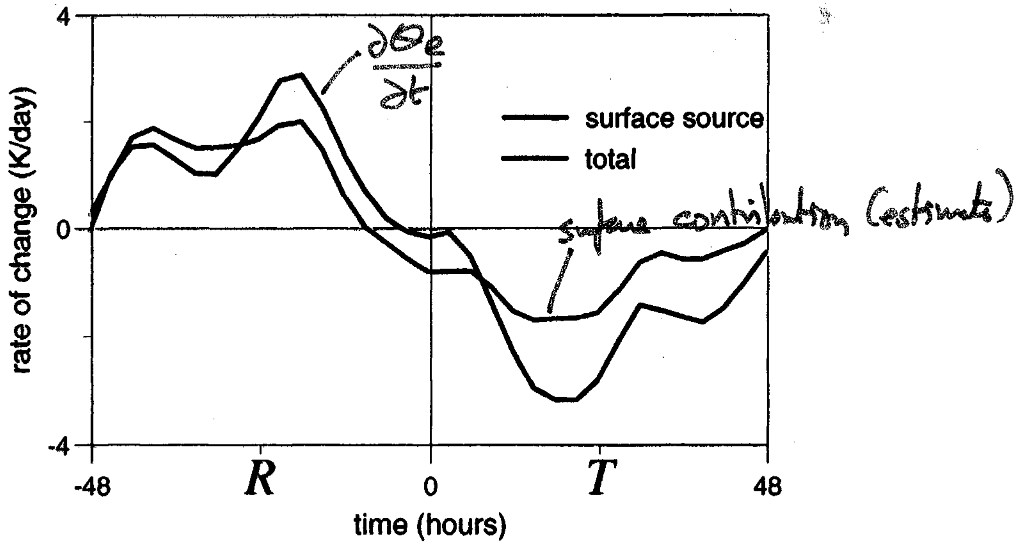

considers the direct effect of the diabatic heating on wave growth at the level of the AEJ. ... on both the heating profile and the phase of the wave where the heating occurs. If the heating reinforced the temperature structure depicted in Figure 9 then the wave would be expected to grow. If it opposed the

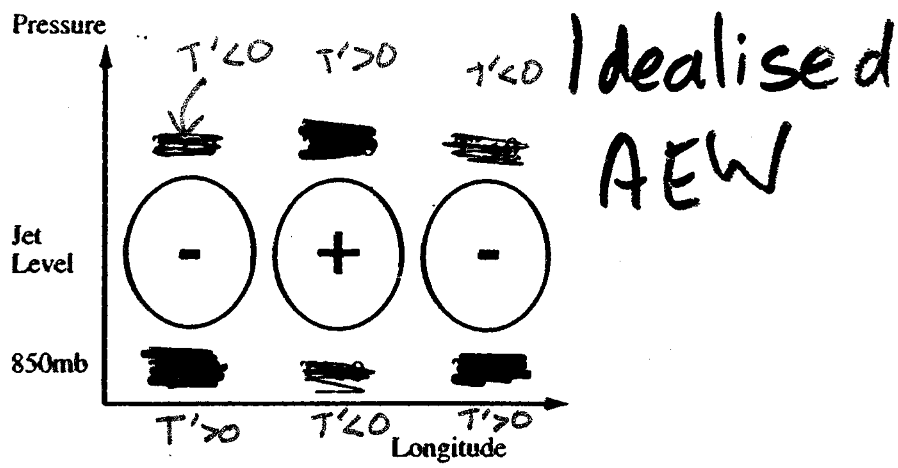

Figure 9. Schematic showing pressure-longitude section of relative vorticity anomalies and associated temperature anomalies in an idealised easterly wave. Maximum amplitudes are assumed at the level of the AEJ and the sign of the relative vorticity anomaly is given by a + and a − sign. The sign of the temperature anomalies is consistent with thermal wind balance. The observed zonal wavelength (see Reed *et al.*, 1977), given here by the distance between the two negative anomalies, typically varies between about 20° and 40°

Thorncroft + Rowell 1998

speculation about role of diabatic heating on AEWs — convection

...rface can reinforce temperature anomalies

Surface flux variability makes substantial contribution to low level heat and moisture variability across wave

How might this affect wave?

θ

Temperature anomalies beneath African Easterly Jet enhanced - this may strengthen waves at jet level

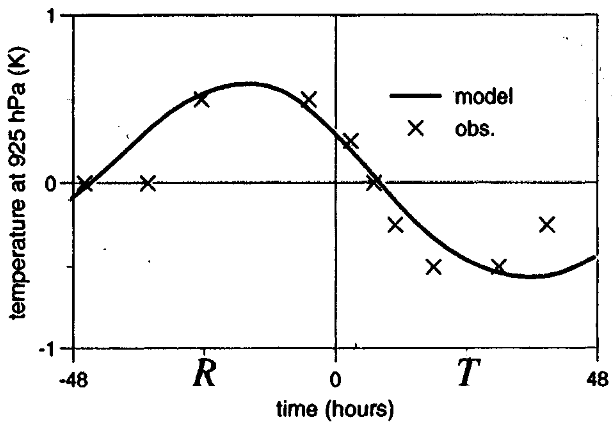

θe

Surface moistening may influence timing of convection associated with wave